Graz University of Technology
Erzherzog-Johann-University

BIOCENTER INNSBRUCK

Investigation of the enigmatic role of Caspase 2 in response to DNA damage in mammalian tumour cells

Master Thesis of Birgit Luef

Submitted in partial fulfilment of the requirements

for the degree of Master of Science

at the Faculty of Technical Chemistry, Chemical Process Engineering and Biotechnology

at Graz University of Technology

Supervisor:

Prof. Dr. Peter Macheroux

Institute of Biochemistry

Graz University of Technology

Advisor:

Ao. Prof. Dr. Stephan Geley

Division of Molecular Pathophysiology

Biocenter Innsbruck

Medical University Innsbruck

Graz, 2011

EIDESSTATTLICHE ERKLÄRUNG

Ich erkläre an Eides statt, dass ich die vorliegende Arbeit selbstständig verfasst, andere als die angegebenen Quellen/Hilfsmittel nicht benutzt, und die den benutzten Quellen wörtlich und inhaltlich entnommene Stellen als solche kenntlich gemacht habe.

Graz, am ……………………….…   …………….…….……………………………..
                                                                                    (Unterschrift)

STATUTORY DECLARATION

I declare that I have authored this thesis independently, that I have not used other than the declared sources / resources, and that I have explicitly marked all material which has been quoted either literally or by content from the used sources.

……………………………   …………….…………………………………..
          date   (signature)

Acknowledgments

I would like to express my gratitude to Ao. Prof. Dr. Stephan Geley for giving me the opportunity to do my master thesis in his work group, for financial support and the chance to work on such an interesting research project. Moreover, I want to thank him for his continuous support, for confidence und for his excellent advices.

Special thanks go to my lab team of "Division of Molecular Pathophysiology", especially to Veronika who introduced me to mammalian cell culture, special cell biological techniques and supported me throughout my lab work.

Reini was more like a mentor rather than just a colleague. I want to thank him for his assistance in microscopy and in daily work, for taking time discussing results, designing further experiments and for answering all my scientific questions.

I appreciated an outstanding training in the lab of Dr. Stephan Geley, which is related to a pleasant working atmosphere, brilliant colleagues and an excellent advisor.

Special thanks go to the lab team of Prof. Dr. Andreas Villunger for his collaboration. In particular, Lukas for his support in optimizing the staining protocol for flow cytometry analysis and Claudia for discussions concerning caspase 2.

I also want to thank Günther for his patience and introduction to flow cytometry.

Furthermore, I want to express my gratitude to Prof. Dr. Peter Macheroux for giving me the possibility to do my practical work abroad and for his encouragement throughout my studies.

Grateful thanks are given to my dear family for their support throughout my studies, for always believing in me and for enabling my studies at the university.

Abstract

Caspase 2 is one of the most evolutionarily conserved caspases, yet its biological function remains enigmatic. Caspase 2 has been shown to become activated in response to DNA damage and has been implicated in mediating the DNA damage-induced G2/M checkpoint. Caspase 2 has also been postulated to function as a tumour suppressor, at least in certain model of murine tumorigenesis. Surprisingly, however, caspase 2 deficient mice show only very mild phenotypes.

In this thesis I focused on the influence of caspase 2 on cell cycle regulation in mammalian tumour cells upon DNA damage. I established and used conditional RNAi cell lines that were synchronized using a double thymidine block (DTB) and treated with ionizing radiation in G2-phase. By monitoring the onset of mitosis in treated as well as untreated control cells I could not find evidence that caspase 2 is essential for the G2/M checkpoint.

Zusammenfassung

Caspase 2 ist eine der am längsten bekanntesten Caspasen, zugleich aber auch die am wenigsten erforschte. Es konnte gezeigt werden, dass Caspase 2 durch DNA-Schäden aktiviert wird dann eine Funktion im G2/M checkpoint übernimmt. Unter anderem wurde Caspase 2 durch Experimente mit Mäusen als Tumorsuppressor erkannt. Wegen geringer Auswirkungen auf den Phänotyp bei Caspase-2-knock-out-Mäusen und fehlender spezifischer Substrate bleibt die Funktion weiterhin ein Rätsel.

Um den Einfluss von Caspase 2 im Zellzyklus humaner Tumorzellen zu untersuchen, wurden konditionale RNAi Zelllinien eingesetzt. Besonderes Augenmerk wurde dabei auf den G2/M checkpoint und dessen Verhalten gegenüber DNA Schäden gelegt. Die Zellen wurden dafür mittels doppeltem Thymidinblock synchronisiert und in der G2-Phase mit γ-Strahlung behandelt. Dieses Experiment bestätigt, dass Caspase 2 keine relevante Funktion am G2/M Übergang einnimmt.

Abbreviations

AA	acryl amide
APS	ammonium peroxodisulfate
ATM	ataxia telangiectasia-mutated
ATR	ATM and Rad-3 related
Bis	N,N'-Methylenebisacrylamide
Casp2	caspase 2
CDK	cyclin dependent kinase
Ced3	cell death protein 3
Chk1	checkpoint-kinase 1
Chk2	checkpoint-kinase 2
CKI	cyclin dependent kinase inhibitor
DMEM	Dulbecco's modified eagle medium
DMSO	Dimethylsulfoxide
DNA-Paces	DNA-dependent protein kinase catalytic subunit
DTB	double thymidine block
ECL	enhanced chemiluminescence
EtOH	ethanol
FCS	fetal calf serum
FITC	fluorescein isothiocyanate
FL	full length
GAPDH	glyceraldehyd-3-phosphate dehydrogenase
GFP	green fluorescence protein
Gy	gray
H	histone
HRP	horseradish peroxidase
ICE	interleucin-1β-converting enzyme
Ich1	ICE and CED-3 homologue 1
IR	ionizing radiation
KO	knock-out
ME	mercaptoethanol
MEFs	mouse embryonic fibroblasts

NLS	nuclear localization signal
Noc	nocodazole
PBS	phosphate buffered saline
PI	propidium iodide
PIDD	p53-induced protein with a dead-domain
puro	puromycin
RAIDD	receptor-interacting protein-associated ICH-1/CED3 homologous protein with death domain
rcf	relative centrifugal force
RIPA	RadioImmuno-Precipitation Assay
RNA	ribonucleotidacid
RNAi	RNA interference
rpm	rounds per minute
shRNA	short hairpin RNA
siRNA	small interfering RNA
SSB	SDS sample buffer
TCA	trichloroacetic acid
TEMED	N,N,N',N'-Tetramethylethylenediamine
tetR	tet-Repressor
THT	TetO7-H1-TetA
Tris	tris(hydroxymethyl)-aminomethan
V	volt

Table of contents

1 Introduction

1.1 Overview of the cell cycle

Cellular reproduction, which is the fundamental mechanism of life, depends on the exact duplication of chromosomes and their equal segregation into the genetically identical daughter cells. The cell division cycle, or short, cell cycle, is comprised of 4 phases, which are defined by the time period a cell requires to duplicates its DNA (S-phase) and to segregate it during cell division (M-phase). These two phases are timely separated from each other by so-called gap (G) phases. The transition between these different cell cycle phases is governed by a highly complex control system. This system basically consists of two layers, a central cell cycle machinery, or cell cycle clock, and control layers that coordinate the activity central machinery with extra- and intracellular signals. A defective control system can result in unfaithful DNA synthesis and segregation as well as to unconstrained cellular proliferation, which can lead to severe diseases like cancer. Figure 1 gives an overview of the 4 phases of the eukaryotic cell cycle.

In G1-phase between mitosis and DNA-synthesis, the cell is sensitive to extracellular proliferative signals, such as growth factors, nutrients and signals emitted by neighbouring cells. These signals trigger cellular growth as well as re-entry into the proliferative state. If environmental conditions are unfavourable (limited nutrients or growth factors) the cell exits the cell division cycle and goes into G0 phase, the resting state. Cells can reside there up to years but can be re-called into proliferation. If growth factors and nutrients are sufficiently abundant, the cell grows and trespasses the so-called restriction (R) point (G1/S checkpoint), beyond which cell cycle progression becomes cell autonomous and cells enter into S-phase. During S-phase, replication of nuclear DNA occurs which takes around 6-10 hours in mammalian cells. After DNA replication, the newly synthesized chromosomes have to be checked for their integrity, by eliminating replication errors, DNA fragmentations as well as DNA damage. As long as DNA replication is not completed and DNA damage is detected cells entry into mitosis is inhibited to prevent the generation of mutated progeny. The transition is controlled by the so-called G2/M checkpoint, which has to be inactivated to allow cells to enter M-phase. M-phase consists of nuclear division, i.e., the segregation of chromosomes (mitosis) and cellular division (cytokinesis), which generates the daughter cells. Chromosome segregation starts with the assembly of the replicated and paired sister chromatids into the mitotic spindle which their splitting during ana- and telophase.

Cytokinesis is initiated during telophase by the assembly of a contractile ring beneath the cellular membrane that is formed between the two sets of segregating chromosomes. Contraction of this ring during telophase initiates cytokinesis. Anaphase and onset of cytokinesis are also coordinated by a checkpoint that monitors the formation of the mitotic spindle (the so-called spindle checkpoint). Upon inactivation of this checkpoint, the cell cycle machinery is reset and the cells returns to interphase (G1-phase) [1].
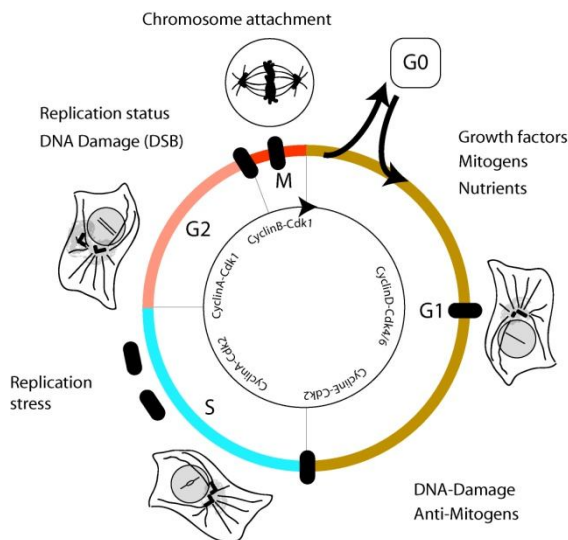

Figure 1: Overview of the eukaryotic cell division cycle. The cell division cycle of somatic cells consists of 4 phases: G1-phase, S-phase, G2-phase and M-phase. The black bars mark the so-called "checkpoints", which are defined points at which cell cycle progression can be halted. Somatic cells can exit the cell division cycle in G1-phase to either differentiated or retrieve from the proliferative state to enter quiescence or in G2-phase (e.g. oocytes). The standard cell division cycle lasts approximately 24 hours with S- and M-phase taking about 8 and 1 hour, respectively. Cells spend most of their time in G1-phase, which is the most variable one between different cell types and cellular activation states. For further details see text [picture thankfully provided by Dr. Stephan Geley].

1.2 DNA is packaged into chromatin

Within the nucleus, DNA is associated with histone and non-histone proteins. Histones H2A, H2B, H3 and H4 form an octamer with DNA wrapped around and hence form the nucleosome, the basic structural unit of chromatin. The N-terminal tails of histones protrudes out of the nucleosome and are targeted by many signalling pathways that generate the so-called histone code, or epigenetic signature, which defines the functional state of chromatin. During mitosis, DNA is hypercondensed to allow the long DNA molecules to be effectively segregated into the two daughter cells. This condensation is associated with phosphorylation of serine 10 of histone H3. Because serine 10 phosphorylation is restricted to mitosis, mitotic cells can be identified by detection of this defined posttranslational modification.

1.3 DNA damage checkpoint control in eukaryotic cell division cycle

The cell division cycle is controlled by cyclin dependent kinases (CDKs), which are regulated by association with cyclins, phosphorylation by upstream kinases and binding to CDK inhibitory proteins. Cyclins activate Cdks and additionally are responsible for the substrate specificity of a defined cyclin-Cdk-complex [1]. Cyclins oscillate during the cell division cycle as a result of regulated synthesis as well as – and importantly – regulated proteolysis. The cyclical changes in cyclin levels are the basis for oscillatory behaviour of CDK activities, which control progression through the cell division cycle. This system is controlled by positive and negative feedback loops which generate an autonomous 'clock'. As already mentioned above, this core cell cycle machinery is controlled by so-called checkpoint mechanisms, which integrate several extra- and intracellular cues and control the activation of CDKs at defined points during the cell division cycle.

As can be seen in Figure 1, the cell division cycle contains 4 major checkpoints that control entry into S-phase, progression through S-phase and entry into mitosis. The forth checkpoints operates in mitosis and governs the onset of anaphase and exit from mitosis by coordinating spindle assembly with the inactivation of CDK activity. If these "control systems" detects any defects inside or outside the cell, it halts the cell cycle by blocking the activation of downstream CDKs or maintaining CDK activity and, thus, halts cell cycle progression. Figure 2 summarizes the key components of the cell cycle regulator proteins and important substrates.
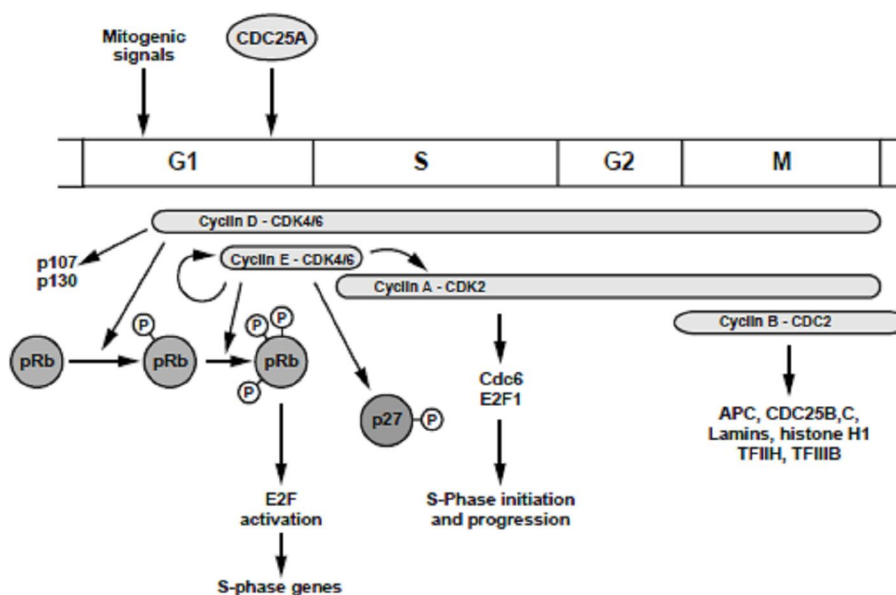

Figure 2: Cell cycle phase specific activation of Cdks and important substrates. The figure shows cyclin-Cdk-complexes that are responsible for cell cycle progression. CyclinD-Cdk4/6-complex becomes activated through mitogenic signals, phosphorylates pRb (Retinoblastoma protein) and pRb-related proteins such as p107

and p130. This phosphorylation blocks the inhibitors action of pRb on the E2F transcription factors, which leads to the induction of cyclinE. After cyclinE-Cdk2-complex formation, necessary for crossing the restriction point, key target substrates are phosphorylated, such as the cyclin-dependent kinase inhibitor protein (CKI) p27, which leads to its degradation by the proteasomal pathway. Further phosphorylation of pRb causes the induction of other genes required for the execution of DNA synthesis. Among those targets are histones, the MCM proteins, as well as cell cycle regulators, such as cyclinA, which is required for progression through S-phase and for the onset of mitosis. Just before the onset of mitosis, the cytoplasmatic and inactive pool of cyclinB-Cdc2 (also known as Cdk1) becomes activated by CDC25 phosphatase. The sudden translocation of Cdk1 into the nucleus and its sudden rise in activity then triggers mitosis, which starts with the dissolution of the nuclear envelope, which is triggered by the phosphorylation of the nuclear lamins [18]. Cdk1 activity is required for the formation of the mitotic spindle. Exit from mitosis is triggered by the activation of a mitotic ubiquitin ligase, which polyubiquitylates mitotic cyclins and thus terminates Cdk1 activity.

Checkpoint proteins monitor the cellular state and feed into a key regulatory point. For example, the absence of sufficient nutrients, aberrant oncogenic signalling, DNA damage, etc. can be detected throughout the cell division cycle but activate pathways that will block cell cycle during late G1-phase to prevent further proliferation. Thus, checkpoints, are not control points that operate at certain times during the cell cycle but rather continuous monitoring processes that affect critical transition points. The first of such transition points lies in late G1-phase and is also called the restriction point.

The restriction point is due to the cell cycle inhibitory properties of pRb as well as the CDKi family of proteins. Both proliferation constraints can be overcome by sufficient amounts of cyclinE-Cdk2 activity [1]. Upon DNA damage, ATM (ataxia telangiectasia-mutated) and ATR (ATM and Rad-3 related), both serine/threonine kinases, get activated and signals are transduced to activate checkpoint-kinase 1 (Chk1) and checkpoint-kinase 2 (Chk2). These phosphorylated kinases thus destabilize CDC25a phosphatase, which is required to activate Cdk2 by removal of the inhibitory phosphate residues at Thr14 and Tyr15. Inhibition of Cdk2 prevents entry into as well as progression through S-phase and thus prevents the fixation of DNA damage as mutation (see Figure 3) [18].
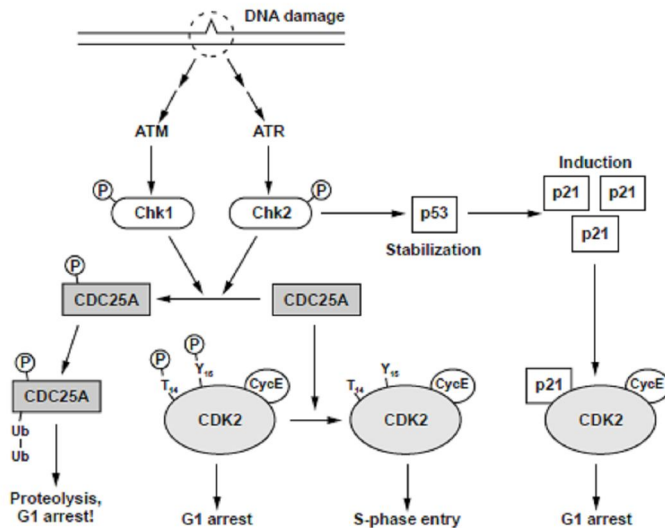
Figure 3: Scheme of the G1 DNA damage checkpoint [18]. DNA damage activates ATM and ATR, the upstream regulators of Chk1 and Chk2. An ultrafast mechanism inhibits Cdk2 activity via degradation of CDC25a, while a second slower but longer lasting pathway is triggered by activation of p53 and induction of the cyclin-dependent kinase inhibitor protein (CKI) p21CIP1. To simplify this scheme not all proteins involved in this DNA damage signalling pathway are depicted, just the most important adaptor and effector proteins.

Ongoing DNA replication also activates the ATR dependent checkpoint in a manner that will prevent entry into mitosis unless DNA is fully replicated. This is achieved by preventing the activation of cyclinB and Cdk1, which in turn activate proteins responsible for mitotic spindle assembly, chromosome condensation and reorganization of the cytoskeleton [1]. In case of DNA damage, the same set of protein mentioned in Figure 3 get activated and promote phosphorylation of CDC25b/c at defined serine-residues which facilitates the binding of 14-3-3 protein, which causes cytoplasmatic sequestration as well as inhibition of Cdk1 [18].

1.4 The role of caspases in the cell

Caspases are cysteine proteases that cleave their target proteins after an aspartate residue, exist in healthy cells in their inactive form as zymogens. With respect to their function, caspases can be divided into initiator (e.g. caspase-8, -9, -10) and executioner caspases (e.g. caspase-3, -6, -7). Initiator caspases are activated by oligomerization induced by protein-protein interactions that are mediated by their long N-terminal prodomains. Oligomerization induces activation by proteolytic cleavage of two smaller domains, which assembly into a tetramer that is now able to convert the inactive pro-executioner caspases into their active form by proteolysis [2][3][4][5].

Some caspases are essential for the regulation of immune responses (e.g. caspase 1, -4, -5) [18], while others are the central executioners of programmed cell death, or apoptosis. Additionally, caspases, such as caspase 3 and 8, appear to have additional function in cell proliferation and differentiation [10].

Apoptosis can be induced by several stimuli and is required to remove severely damaged, unwanted or dangerous cells. Extracellular death signals are transduced via transmembrane receptors (death receptors) which oligomerize caspase 8 (and 10) close to the plasma membrane in the so-called death inducing signalling complex (DISC) This so-called extrinsic pathway uses "death ligands" such as Fas or the TNF (tumour necrosis factor) to stimulate initiator caspases such as caspase 8 which further activates executioner caspases such as caspase 3. Finally, executioner caspases lead to proteolysis of target substrates (e.g. lamins) that in turn lead to programmed cell death [18].

Cell death can also be triggered from within, by the so-called intrinsic pathway (see Figure 4), in which mitochondria play the key role. Cellular stress, DNA damage, and many other signals mediate the activation of the pro-apoptotic protein Bax that generates pores in the mitochondrial outer membrane to release cytochrome-c from the intermembraneous space. This, in turn, results in the formation of the apoptosome, a multiprotein complex and activation platform of initiator caspase 9. Next, executioner caspases become activated and degrade various cellular substrates (e.g. ICAD, inhibitor of caspase-activated DNAse). The pro-apoptotic (pore forming) ability of Bax is controlled by its ability to interact with anti-apoptotic members of the Bcl-2 family, which block Bax activity by direct binding [18].

Figure 4: Programmed cell death signalling carried out by caspases through 2 defined pathways. On the left hand side, the death receptor pathway is depicted, activated through Fas ligand or TNF. Activation proceeds by binding of the ligand to the transmembrane receptor [TNFR, Fas-receptor (also known as CD95)]. Intramolecular signalling activates caspase 8, which in turn cleaves off the proteolytic domain of caspase 3 and hence degrades specific target substrates. TNF: tumour necrosis factor; TNFR: tumour necrosis factor receptor;
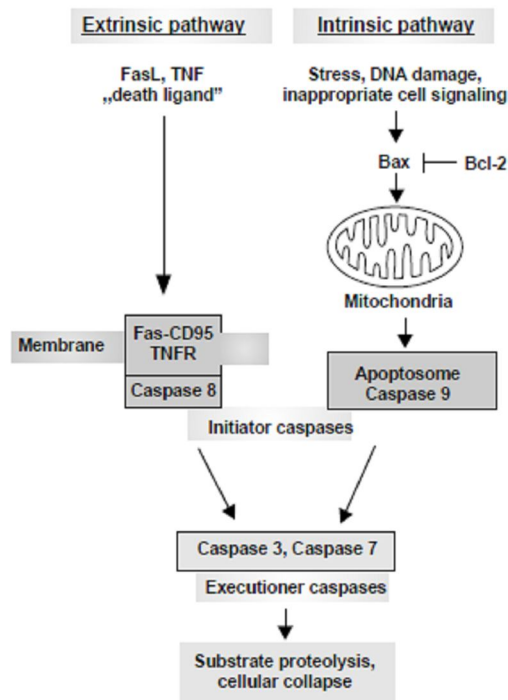
The flow chart of intrinsic pathway is illustrated on the right hand side starting with intracellular signalling and activating of the pro-apoptotic protein Bax. Bax produces pores in the mitochondria outer membrane and thus, induces cytochrome-c release. Cytochrome-c positively regulates the activation of caspase 9 and further stimulates executioner caspases to fulfil the apoptotic program.

1.5   Caspase 2

Caspase 2 was first identified by screening genes that showed upregulation in neural precursor cells and a downregulation during the development of the central nervous system in mice. One of the genes identified in this screen was named *Nedd 2* (neural precursor cell expressed developmentally downregulated gene 2) [14]. The same gene was also identified by others who searched for genes similar to caspase 1 (which is also known as ICE, or interleukin-1β-converting enzyme) and named it *Ich1* (ICE and CED-3 homologue 1) [15]. Later, this gene was renamed caspase 2, which is a 51 kDa protein consisting of a long amino-terminal CARD domain (caspase activation and recruitment domain) and a catalytic domain. Due to the fact that caspase 2 harbours a long prodomain used for protein-protein interactions as caspase 1 and Ced-3, caspase 2 is classified as an initiator caspase [7].

It is one of the most evolutionarily conserved caspases and is thought to play an important role in apoptosis, DNA damage response and tumour suppression. Although several reports have claimed an important function of caspase 2, caspase 2 deficient mice lack an overt phenotype, suggesting that this enzyme is dispensable, at least under the growth conditions of laboratory mice [9] [11][12].

1.5.1 Activation of Caspase 2 *in vivo*

Figure 5 gives an overview of the proposed mechanism of caspase 2 activation. Baliga *et al*. (2004) investigated the mechanism of caspase 2 activation with various recombinant caspase 2 wild type and mutant proteins. Partial activity was observed in a non-cleavable mutant (D333G), suggesting that the first step of caspase 2 activation requires dimerization and not proteolytic processing typical for other caspases. Strikingly, the C320G mutant, which prevents a disulfide-bond formation, showed no catalytic activity. Taken together, dimerization is required for initial acquisition of enzyme activity. Autocatalytic processing by the cleavage at D333 results in the separation of the CARD-p19 fragment and the p14 fragment and stabilization of the tetrameric complex. The fully active state of caspase 2 is generated by removal of the prodomain by D169 cleavage and the intersubunit cleavage at D347 [7].
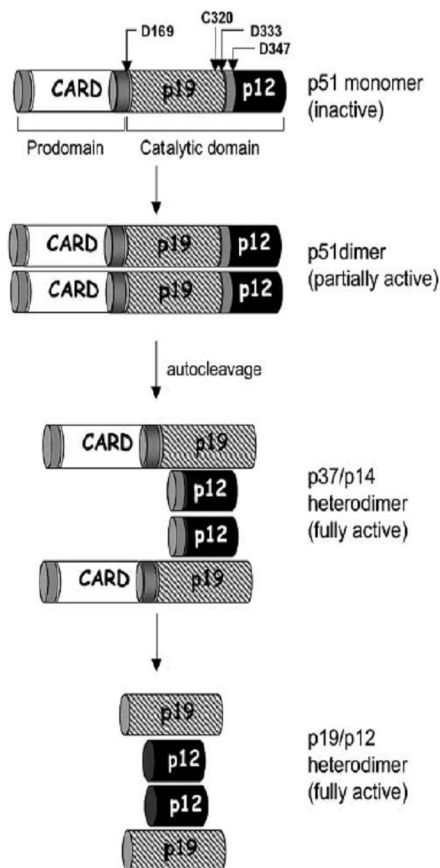
Figure 5: Proposed mechanism of caspase 2 activation *in vivo*. The first scheme illustrates caspase 2 in its inactive, monomeric state with indicated cleavage sites (D169/D333/D347) represented by black arrows. The catalytic residue C320 for disulfide-bond formation is also shown. The prodomain (CARD) is responsible for protein-protein interactions and is thought to bind RAIDD through its CARD domain. Regarding the received data, Baliga *et al*. (2004) suggested that cleavage of caspase 2 is not required for initial activation. Instead dimerization is the first step that leads to a partially active enzyme with subsequent autocatalytic cleavage at D333 further resulting in stabilization of the dimer and a fully active enzyme. Due to similar activation steps in caspase-8 and -9, caspase 2 is thought to belong to initiator caspases. Caspase 2 numbering convention [7]. RAIDD: RIP-associated ICH-1/CED3 homologous protein with death domain.

Activity Assays were carried out with an artificial pentapeptide sequence Ac-VDVAD-amc (Acetyl-Val-Asp-Val-Ala-Asp-Amino-methylcoumarid), which was supposed to be a specific

substrate of caspase 2 [7]. Recent studies, however, revealed that this pentapeptide is a better indicator for caspase 3 than caspases 2 activity [8].

1.5.2 Caspase 2 & its involvement in apoptotic pathways

In 2004, Tinel and Tschopp found that PIDD (p53-induced protein with a dead-domain) binds to RAIDD (receptor-interacting protein-associated ICH-1/CED3 homologous protein with death domain), which in turn results in the activation of caspase 2. The activation of caspase 2 was most prominent in response to genotoxic stress, suggesting a role for caspase 2 in the DNA damage response. Because the PIDD-RAIDD complex was fond to activate caspase 2, the complex was termed PIDDosome"[6]. Interestingly, however, mouse embryonic fibroblasts derived from mice lacking PIDD do not show a defect in caspases 2 activation, suggesting that caspase 2 might be activated by several different pathways [16].

Figure 6: **Proposed scheme of the "Piddosome" – a caspases 2 activation complex.** Caspase 2 gets bound via its N-terminal prodomain to RAIDD, which is the linker protein between PIDD and caspase 2. RAIDD and PIDD interact in this complex via their death domains (DD). Expression of PIDD is related to p53 activation upon DNA damaging treatments [22].

Due to the high sequence similarity of caspase 2 to the *Caenorhabditis elegans* caspase *Ced-3*, it was assumed that caspase 2 knock-out would also result in prevention of apoptosis, as do mutations in the *Ced-3* gene in *C. elegans* [19]. Caspase 2 knock-out mice, however, do not display an overt phenotype [9]. Caspase $2^{-/-}$ female mice show an increased number of germ cells in ovaries and their oocytes were found to be more resistant to genotoxic agents such as doxorubicin, a DNA intercalating chemotherapeutic drug [20].

More detailed analysis of caspase 2-deficient or knock-down cells revealed roles of this caspase in the regulation of apoptosis in response to cytoskeleton disrupting agents, such as vincristine, cytochalasin D and paclitaxel [21].

1.5.3 Role of Caspase 2 in DNA damage response

One special feature of caspase 2 includes its ability to translocate into the nucleus, which is not shared by other caspases [13]. Strikingly, upon DNA damage, caspase 2 translocates from the cytosol to the nucleus [16], a process dependent on an N-terminal nuclear localization signal (NLS). Consistent with that, preliminary data suggest that the activation of caspase 2 is related to a special activation complex, consisting of DNA-dependent kinase catalytic subunit (DNA-PKcs) and PIDD upon DNA damage. The following picture shows the role of caspase 2 in DNA damage signalling resulting in G2/M arrest and non-homologous end joining (NHEJ). In response to double strand breaks (DSB) caused by ionizing radiation, DNA-PKcs gets activated and forms the nuclear caspase 2 activation complex, consisting of DNA-PKcs, PIDD and caspase 2. As such, the activation platform is called the DNA-PKcs-PIDDosome. Shown in Figure 7 DNA-PKcs serves as the adaptor protein for PIDD and caspase 2. PIDD binds through the death-domain (highlighted in dark green) to the amino-terminal region of the protein kinase and caspase 2 gets bound through the prodomain (highlighted in brown) to the C-terminus.

In vitro studies carried out with recombinant PIDD, caspase 2 and DNA-PKcs (purified from HeLa cell nuclei) confirmed that the catalytic subunit of DNA-PK can serve as an adaptor protein for PIDD as well as for caspase 2 [17].

Upon DNA damage, the DNA-PKcs phosphorylates caspase 2 at Ser122 through its kinase activity, which results in activation of caspase 2 and further leads to G2/M arrest. Caspase 2 deficient cells were compared with wild type cells expressing caspase 2 following treatment with DNA damaging agents. Caspase 2 deficient cells failed to arrest efficiently in G2-phase, suggesting that loss of caspase 2 results in a defective G2/M checkpoint. Similar results were obtained with double caspase 2- and *PIDD*-knockout MEFs, immortalized with SV-40 virus [17].

Although caspase 2 is assumed to be involved in apoptosis caused by genotoxic stress, Shi *et al*. (2009) demonstrated that the used cell lines did not show a higher apoptotic rate upon caspase 2 activation through phosphorylation at Ser122 following IR treatment.
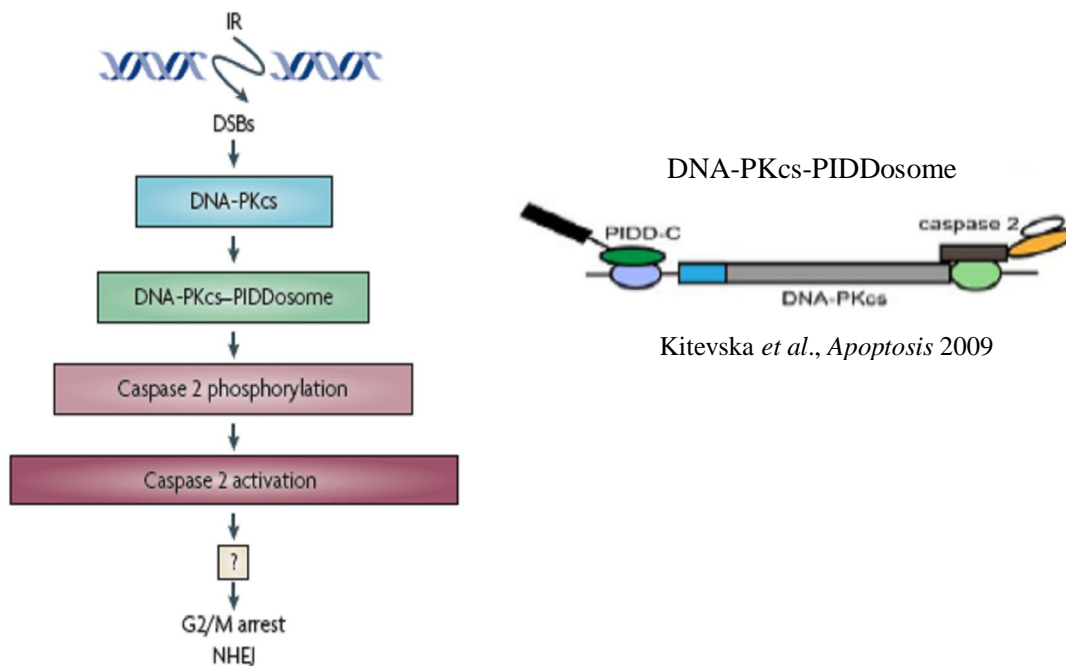
Figure 7: Role of caspase 2 in DNA damage signalling. Upon DNA damage, caused by ionizing radiation (IR) double strand breaks are generated which in turn leads to activation of DNA-PKcs. After forming the activation complex for caspase 2, activation occurs through phosphorylation at Ser122. The downstream targets of caspase 2 that finally leads to G2/M arrest remain unclear so far.
On the right hand side, there is the nuclear DNA-PKcs-PIDDosome presented, consisting of PIDD, DNA-PKcs and caspase 2.

1.5.4 Aim of this master thesis

The aim of my master thesis was to investigate the potential role of caspase 2 in the activation and/or duration of the DNA damage-induced G2/M checkpoint. This checkpoint inhibits entry into mitosis to prevent the transmission of mutations and to provide cells with the opportunity for DNA damage repair. To be able to assess the role of caspase 2 in the G2/M checkpoint, I generated cervical carcinoma HeLa cell lines with stable inducible RNAi to suppress caspase 2 expression. HeLa cells were chosen because these cells allow efficient cell cycle synchronisation, a prerequisite for the biochemical analysis of cellular responses. To achieve stable inducible RNAi, I used lentiviral integration of shRNA expression cassettes. These cassettes consisted of a conditional doxycycline regulated promoter and a shRNA encoding sequence. I used 2 different shRNA sequences targeting caspase 2 and one targeting firefly luciferase, as a control for non-specific RNAi effects. To achieve conditional RNAi, I used two different systems, which were both based on the doxycycline-adjustable THT promoter. In the first system the TetR repressor required to silence the THT promoter was expressed

from the same lentiviral construct as the THT-driven shRNA gene. In the second system, I used a HeLa cell line that expressed TetR independently from the shRNA lentiviral construct.

2 Materials

2.1 General reagents and materials

Table 1: General reagents and materials

Substances	Manufacturer
0.25% Trypsin-EDTA solution	Sigma, Austria
1000 U Penicillin/mL; 1000 U Streptomycin/mL	Lonza, France
2% Bisacrylamide	Merck, Germany
2-Mercaptoethanol	Sigma, Austria
30% AA (Rotiphorese Gel A)	Roth
Amersham Hyperfilm ECL	GE Healthcare
Ammonium persulfate (APS)	Serva, Austria
Bovine serum albumine	Sigma, Austria
Bromphenol Blue	Merck, Germany
Complete tablets, EDTA free	Roche, Austria
Dimethylsulfoxide (DMSO)	Roth
DMEM high glucose (4.5 g/L)	PAA Laboratories, Germany
Doxycycline	Sigma, Austria
Dried skimmed milk powder	Marvel, GB
ECL	Pierce, Austria
Ethanol, absolut	Merck, Germany
Ethylenediaminetetraacetic acid (EDTA)	Sigma, Austria
Fetal Bovine Serum Gold (FCS)	PAA Laboratories, Germany
Glycerol	Merck, Germany
Glycine	USB, USA
HT1.000G Plus Medical X-ray film	AGFA
Igepal CA-630 (NP40)	Sigma, Austria
K_2HPO_4 x 3 H_2O	Merck, Germany
KCl	Merck, Germany
KH_2PO_4	Merck, Germany
Metafectene^{TM} Transfection Reagent	Biontex, Germany
Na_2HPO_4	Merck, Germany
NaCl	Merck, Germany
Na-deoxycholate	Sigma, Austria
Nitrocellulose membrane 0.45 μm	Whatman, UK
Nocodazole	Sigma, Austria
OPTI-MEM I + GlutaMAX 1x	Invitrogen,
Page Ruler Plus Prestained Protein Ladder	Fermentas

Penicillin/Streptomycin	Lonza, France	
Ponceau S Red	Sigma, Austria	
Propidium iodide	Sigma, Austria	
Protein Assay Reagent (Bradford, 5x)	Bio-Rad, USA	
Protogel = Rotiphorese Gel 30 = 37.5:1 30% AA-stock solution mixed with 0.8% Bis)	Roth	
Puromycin	Sigma, Austria	
RNAse A	Sigma, Austria	
SDS	Roth	
Temed	Invitrogen	
Thymidine	Sigma, Austria	
Trishydroxymethyl-aminomethan	Merck, Germany	
Triton X-100	Sigma, Austria	

2.2 General buffers and solutions

Table 2: General buffers and solutions

Buffer/Solution	Substance(s)	Final concentration
-Ab medium	DMEM (high glucose 4.5 g/L) FCS L-Glutamine	10 % 2 mM
Bradford Assay	Dye reagent concentrate Aqua bidest.	1/5 4/5
Culture medium	DMEM (high glucose 4.5 g/L) FCS Penicillin/Streptomycin L-Glutamin	10 % 1 % 2 mM
DNA staining solution for flow cytometry	PBS RNAse A Propidium Iodide (PI)	0.1 mg/mL 25 μg/mL
ECL	Luminol Enhancer Solution Peroxide Solution	mix 1:1
FACS buffer	EDTA KCl KH_2PO_4 Na_2HPO_4 LiCl	25 mM 75 mM 38 mM 333 mM 200 μM
	Mix all reagents listed above in 3-4 L aqua deion. and add NaCl to a f.c. 2.8 mM. Then fill up to 20 L with aqua deion. (pH 7.1 – 7.3).	
Freezing medium	FCS DMSO	90 % (v/v) 10 % (v/v)
Membran blocking	dried skimmed milk powder	10 % (w/v)

buffer	washing buffer	90 % (v/v)
Phosphate buffered saline (PBS)	NaCl	24 g
	KCl	0.75 g
	Na_2HPO_4	4.29 g
	KH_2PO_4	0.75 g
	Fill up 3 L with aqua deion. (pH 7.2 – 7.4) and autoclave it.	
Ponceau S	Ponceau S	0.3 %
	3 % TCA	
Protogel	30% AA	37.5:1
	0.8% Bis	
RIPA buffer	NaCl	150 mM
	Tris	50 mM
	NP40	1 %
	Na-deoxycholate	0.5 %
	SDS	0.1 %
	Per 50mL of this buffer add 1 tablet of Complete protease inhibitor cocktail – aliquote and store at -20 °C.	
SDS sample buffer (4x SSB)	SDS	8 %
	Tris-HCl, pH 6.8	320 mM
	Glycerol	40 %
	Bromophenol blue	try 1 mL of 0.2% w/v stock in EtOH abs.
	Mix with aqua deion. and add β-mercaptoethanol (f.c. 20%) just before use. To prepare 1x SSB work solution dilute the 4x SSB with aqua bidest. and add β-mercaptoethanol (f.c. 5%) just before use.	
SDS-PAGE Running Buffer	Glycine	288 g
	Tris base	20 g
	10 % SDS	100 mL
	Fill up to 10 L with aqua dest.	
12.5 % Separating gel	Aqua bidest.	1.6 mL
	30% Protogel	2.0 mL
	1.5 mM Tris-HCl pH 8.8	1.3 mL
	10% APS	50 μL
	TEMED	5 μL
5 % Stacking gel	30 % AA	16.66 mL
	2 % Bis	6.40 mL
	1.5 mM Tris-HCl pH 6.8	12.50 mL
	Aqua bidest.	64.44 mL
	The stacking gel can be prepared in advance with all reagents listed in the column except 10% APS and TEMED and stored at 4 °C. To 2 mL of the stacking gel mix, add 25 μL 10% APS and 2.5 μL TEMED. Mix well and pour the mix on top of the separating gel.	
Transferbuffer 1x	Glycine	14,4 g
	Tris	3 g
	MeOH	20 %
	SDS	0.1 %

	Fill up to 1 L with aqua deion.	
Trypsin 1x	0.25% Trypsin-EDTA solution	20 % (v/v)
	Versene	80 % (v/v)
Versene	PBS	
	EDTA	1 mM
Washing buffer	10x PBS	
	NP40	0.5 %
	Dilute with aqua deion.	
Washing buffer for flow cytometry (WB)	PBS	
	BSA	1 %

2.3 Cell lines

All cell lines were used as a bulk unless stated otherwise.

Table 3: used cell lines

Cell lines	Description
HeLa	Human epithelial cervix carcinoma cell line; established from **He**nrietta **La**cks, a 31 year old afro-american woman
HeLa-Caspase2-1sh-tetR-GFP	HeLa cells infected with Caspase2-1sh-tetR-GFP
HeLa-Caspase2-3sh-tetR-GFP	HeLa cells infected with Caspase2-3sh-tetR-GFP
HeLa-Luciferasesh-tetR-GFP	HeLa cells infected with Luciferasesh-tetR-GFP
HeLa-tetRA5	Single clone; infected with tetR
HeLa-tetRA5-Caspase2-1sh-puro	Bulk after Puromycin selection; infected with Caspase2-1sh-puro.
HeLa-tetRA5-Caspase2-1sh-puro+	Bulk after Puromycin selection; infected with Caspase2-1sh-puro. permanent treated with 500 ng/mL doxycycline
HeLa-tetRA5-Caspase2-3sh-puro	Bulk after Puromycin selection; infected with Caspase2-3sh-puro.
HeLa-tetRA5-Caspase2-3sh-puro+	Bulk after Puromycin selection; infected with Caspase2-3sh-puro. permanent treated with 500 ng/mL doxycycline
HeLa-tetRA5-Luciferasesh-puro	Luciferase was used as a negative control (off-target) Bulk after Puromycin selection; infected with Luciferasesh-puro.
HeLa-tetRA5-Luciferasesh-puro+	permanent treated with 500 ng/mL doxycycline
HEK 293T	Human embryonic kidney cell line; established from a human primary embryonic kidney

	transformed by adenovirus type 5 protein E1a; producer cell line for lentivirus production;
MEFs wt	Mouse embryonic fibroblast cell line; immortalized with SV40 large T
Caspase 2 KO MEFs	Mouse embryonic fibroblast cell line; Caspase 2 knock-out

2.4 Plasmids

The following plasmids were already generated and I got them ready to use.

Table 4: used plasmids

Plasmids	Features
pHR-THTIII-Caspase2-1shRNA-tetR-GFP	shRNA-sequence # 1 targeting caspase 2; tet-repressor is expressed as a fusion protein with GFP
pHR-THTIII-Caspase2-3shRNA-tetR-GFP	shRNA-sequence # 3 targeting caspase 2; tet-repressor is expressed as a fusion protein with GFP
pHR-THTIII-Luciferase shRNA-tetR-GFP	shRNA-sequence targeting Luciferase; tet-repressor is expressed as a fusion protein with GFP
pHR'-THTIII-Caspase2-1shRNA-puro	shRNA sequence # 1 targeting caspase 2; Puromycin was used as a selection marker
pHR'-THT-Caspase2-3shRNA-puro	shRNA sequence # 3 targeting caspase 2; Puromycin was used as a selection marker
pHR'-THT-LuciferaseshRNA-puro	shRNA sequence targeting Luciferase; Puromycin was used as a selection marker
psPAX2	Packaging plasmid carrying lentivirus genes
pVSV-G	Expression of vesicular stomatitis virus glycoprotein for "pseudo-typing"

2.5 shRNA sequences

The shRNA sequences listed below were already purchased by MWG and ready to use.

Table 5: shRNA sequences

Target protein	shRNA sequence
Caspase 2 #1	5' GCCCAAGCCTACAGAACAA
Caspase 2 # 3	5' AGACATGATATGCGGCTAT
Firefly luciferase	5' CTTACGCTGAGTACTTCGA

2.6 Antibody catalogue

Listed antibodies were used for Immunoblotting (IB) as well as for Immunofluorescence (IF) experiments. Primary antibodies as well as secondary Ab's were diluted in membrane blocking buffer.

Table 6: Primary antibodies

Specificity	Clone	MW (kDa)	Dilution	Species	Used for	Manufacturer
Caspase 2	11B4	51, 37	1:1000	Rat	IB	Alexis
Caspase 2	homemade (20 µg)	51, 37	1:500	Rat	IB	Australia
GAPDH	6C5, High TestLtd (3.2 mg/mL)	35.9	1:10000	Mouse	IB	
Cyclin B1	mAb, V152 (1 mg/mL)	55	1:200	Mouse	IB	
Phospho-H3 (Ser10)[1]	polyclonal	17	1:500	Rabbit	IB, IF	Upstate/Millipore
Phospho H3-FITC[1]	mAb, 3H10	17	1:150	Mouse	IF	Millipore
Phospho-H2A.X (Ser139)[2]		17	1:100	Rabbit	IB	Cell signalling Cat.No. 2577S

[1] Mitosis Marker, [2] DNA double-strand break marker

Table 7: Secondary antibodies

Specificity	Dilution	Species	Used for	Manufacturer
HRP-anti-Mouse	1:3000	goat	IB	Dako, Amersham
HRP-anti-Rabbit	1:3000	donkey	IB	Dako, Amersham
HRP-anti-Rat H+L	1:2000		IB	
Alexa488-anti-Rabbit	1:1000	goat	IF	Molecular Probes = Invitrogen
Alexa647-anti-Mouse	1:1000	goat	IF	Molecular Probes
Alexa546-anti-Mouse	1:1000		IF	Molecular Probes
DNA stains:				
Hoechst 33342	1µg/mL		IF	Sigma

2.7 Kits

ECL was purchased from Pierce and used according to the manufacturer's manual.

2.8 Equipment

Table 8: Technical devices

Purpose of use	Device	Manufacturer
Flow cytometry	FACScan	Becton Dickinson
Immunoblotting	TE 77PWR roller mixer SRT9	Amersham Biosciences Stuart
Sonification	U200S control (cycle 0.5; amplitude 50%)	IKA Labortechnik
Plate reader	Sunrise	Tecoa (Programme: Magellan)
Developer	Curix 60	AGFA
Cell culture	Incubator Laminar Flow Cabinet 10 cm tissue culture dishes 6 well plates 35 mm tissue culture dishes Cryo.S, PP, with screw cap 15 mL falcon tubes 50 mL falcon tubes	Binder Thermo Scientific Sarstedt, USA Becton Dickinson Sarstedt, USA Greiner bio-one, Germany BD Falcon, USA BD Falcon, USA
Centrifuges	Eppendorf Centrifuge 5415R GPR Centrifuge Sorvall RT7 Plus	Eppendorf Beckman Kendro
Haemocytometer counting chamber	Neubauer improved	Marienfeld, Germany
Microscope	ZEISS *Axiovert 200M*	Zeiss, Jena, Germany
	ZEISS Axio Observer A1	Zeiss, Jena, Germany

3 Methods

3.1 Cell culture

3.1.1 Thawing cells

Cryo tubes containing 10^6 cells in freezing medium were removed form -80 °C storage, briefly thawed in a 37 °C waterbath, diluted in 20 mL culture medium (DMEM) and pelleted (5 min., 1200 rpm). After removal of the supernatant, the cells were resuspended in fresh culture medium, plated on a 10 cm cell culture dish and incubated in a water saturated environment (37 °C, 5 % CO_2).

3.1.2 Human and mouse cell culture

Serial passaging of cells required detachment of cells from their substrate by trypsination. After removal of the culture medium, cells were washed in sterile PBS and 2 mL Trypsin solution added per 10 cm plate and incubated at 37 °C for 5 to 10 minutes. Trypsination was stopped by adding 8 ml culture medium and the appropriate volume of cell suspension was transferred in a dish supplemented with culture medium according to the experimental procedure.

3.1.3 Counting cells

To seed a defined number of cells per dish, cells were washed once in autoclaved PBS and trypsinized. After thoroughly resuspending the cell suspension, 10 µL were used for cell counting using a haemocytometer counting chamber.
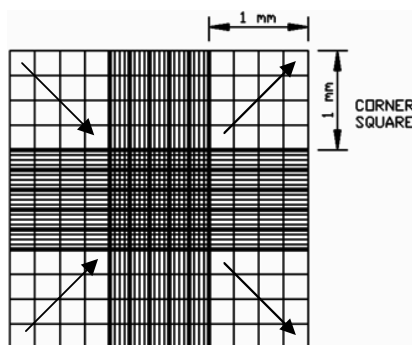

Figure 8: Haemocytometer counting chamber. One corner square (1x1 mm), which consists of 16 little squares, harbours 0.1 µL. I always counted the diagonal of all 4 corner squares (depicted by black arrows) which also end up in 16 little squares. The number of cells was then multiplied by 10 000, which leads to the amount of cells in 1 mL cell-suspension. (Picture was copied from: http://www.google.at/imgres?imgurl=http://www.nexcelom.com/images/Improved-Neubauer-Hemacytometer-Cell-Counting-Grid.gif; accessed at 13.09.2011)

3.1.4 Freezing cells

Cells were grown to confluency in a 10 cm cell culture dish, washed, trypsinized and pelleted by centrifugation (5 min., 1200 rpm, RT). The supernatant was removed and the pellet was resuspended in freezing medium - 800 µL per one 10 cm dish were used. Finally 800 µL were transferred in one cryo tube and frozen to -80 °C, packed in Cryo 1 °C Freezing Container filled with ispropanol to achieve a -1 °C/min. cooling rate

3.2 Cell biological methods

3.2.1 Fixing cells in ethanol for flow cytometry

Cells were harvested by trypsination and pelleted by centrifugation for 5 minutes at 1000 rpm at room temperature. The cells were washed once in PBS and again pelleted by centrifugation for 5 minutes at 3000 rpm. Subsequently, the pellet was resuspended in PBS and ice-cold EtOH (abs.) was added slowly to a final concentration of 70 % (v/v) under gentle vortexing. The fixed cells were stored at 4 °C over night or at -20 °C for prolonged periods.

3.2.2 DNA staining

DNA staining was used for cell cycle analysis as well as for nuclear counterstaining in immunofluorescence experiments. For flow cytometry, fixed cells were pelleted by centrifugation for 5 minutes at 2000 rpm, resuspended in propidium iodide DNA staining solution, transferred into "facs-tubes" and incubated at 37 °C for 25 minutes. Before analysis, the tubes were incubated at 4 °C for at least 10 minutes. Nuclear counterstaining is described in detail below.

3.2.3 Generation of infectious lentiviral particles

All work with lentiviral particles was performed under biological safety 2 conditions. Replication incompentent infectious lentiviral particles were generated by co-expression of viral genes and the viral genome in HEK293 packaging cells in the presence of VSV-G for pseudotyping.

The packaging plasmid carries the viral genes *gag*, which encodes the capsid proteins, and *pol* that encodes reverse transcriptase and integrase. The vector plasmid, pHR'-SIN, contains the psi (ψ) sequence for packaging viral RNA into virus capsids and the transgene located in between the lentiviral LTRs for target cell integration. The Vesicular Stomatitis Virus G

protein (VSV-G) was used for pseudotyping of the viral particles. Genes that are not required for generation of viral particles were deleted from the packaging plasmid (Δ). The lentiviral vector contains a deletion in the 3' LTR (ΔU3) to render it self-inactivating (SIN).
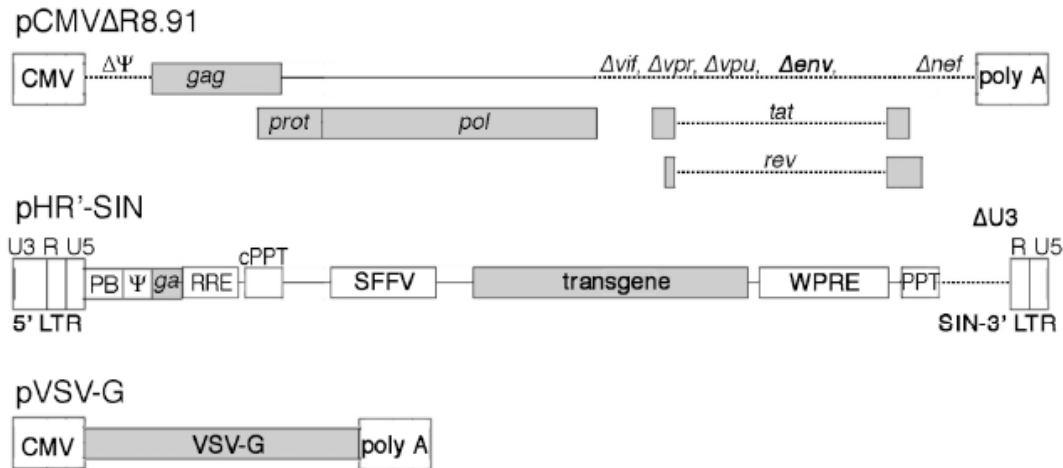

Figure 9: Plasmids for lentivirus production: packaging plasmid (pCMVdeltaR8.91), lentiviral vector pHR'-SIN and the pseudotyping plasmid pVSV-G. These 3 plasmids contain the information required for generating lentiviral particles by transient transfection of packaging cells. Transgene represents the gene of interest. Δ represents a deletion of this sequence [picture thankfully provided by Dr. rer. nat. Reinhard Sigl].

Human embryonic kidney cells (HEK 293T) were used for virus production. Cells were seeded at a density of 0.8 x 10^6 in 6 well plates in culture medium and grown for 18 to 24 hours before transfection. The transfection mix was prepared in two steps: 2 µg pHR-X, 1 µg pSPAX2, and 1 µg pVSV-G were diluted in 100 µL Optimem. In a second tube 12 µL Metafectene were diluted in 100µL Optimem and incubated 5 minutes at room temperature. The contents of both tubes were mixed and incubated for 20 minutes at room temperature. In the meantime, the medium of HEK 293T cells was refreshed with 2 mL –Ab medium. The metafectene-mix was then added dropwise to the cells for 24 to 36 hours at 37°C before the medium was exchanged with 2 mL culture medium. At 48 hours after transfection, the culture medium containing lentiviral particles was harvested (48 h SN) with a syringe and filtered through a 0.45 µm filter. Fresh medium was added to the wells and cells and media harvested 24 hours later (72h SN).

3.2.4 Lentiviral transduction of cells

Target cells (HeLa as well as HeLa-tetRA5) were seeded at a density of 0.4 x 10^6 cells in 6 well plates one day before infection. For infection the medium was exchanged with the 48 h virus containing SN, containing 4 µg/mL polybrene, and incubated for 6 hours at 37 °C. After 6 hours, the same volume of fresh culture medium was added to the target cells. The

following day, a second round of infection with the 72 h virus containing SN was carried out as described above for the 48 h SN. Upon confluency the cells were expanded to a 10 cm dish. Infection efficiency was assessed by fluorescence microscopy (GFP expression) or cells were exposed to a selection agent (e.g. puromycin).

3.2.5 RNA interference

A lentiviral transduction system was used to establish HeLa cells with stable inducible RNAi targeting caspase 2. To achieve this aim, we used a conditional expression system, which consisted of a tetracycline repressible variant of the human H1 RNA gene promoter, called THT promoter that was used to drive the expression of a short hairpin RNA (shRNA) targeting human caspase 2 mRNA. To achieve conditional tetracycline-dependent shRNA gene expression, I used two approaches: in the first approach I used a lentiviral vector that contains the THT promoter as well as TetR, which was encoded by a GFP fusion gene. In the second approach, I used a HeLa cell line that already expressed TetR and I only needed to transduce the cells with a lentiviral construct for expression of the shRNA expression cassette. Both plasmids used to transduce HeLa cells are shown below.
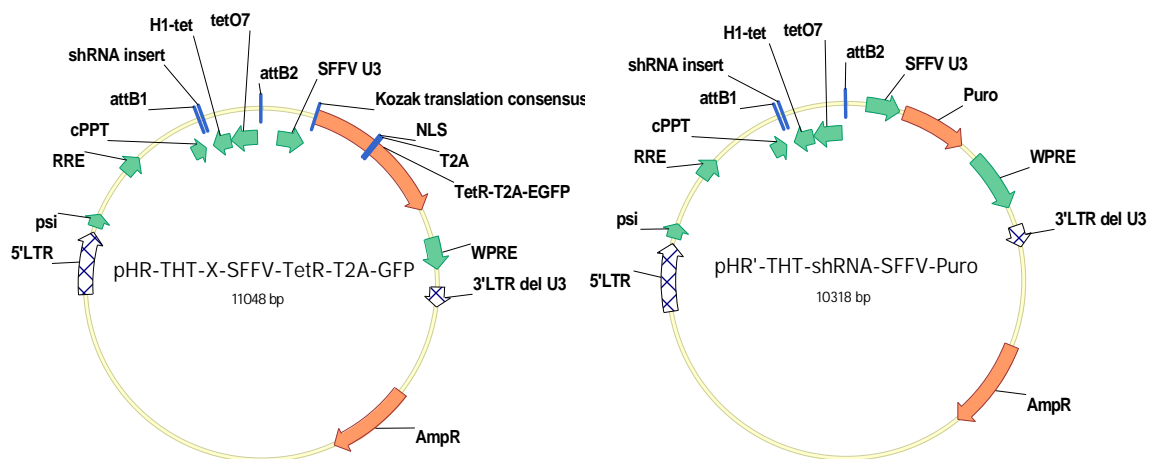

Figure 10: Vectors for transfection. pHR-THTIII-SFFV-TetR-T2A-GFP plasmid is depicted on the left hand side and pHR'-THT-shRNA-SFFV-Puro is presented on the right hand side [provided by Dr. Stephan Geley].
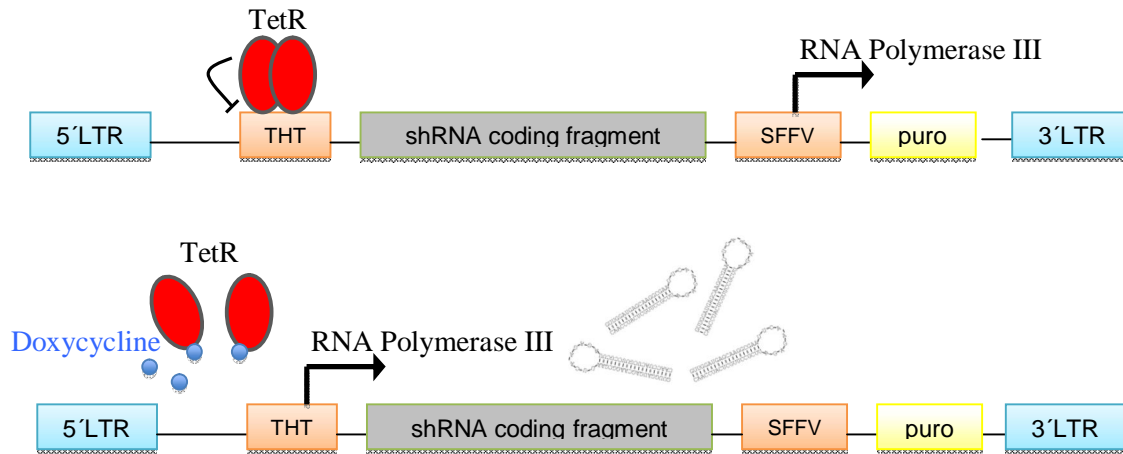
Figure 11: Inducible RNAi system. LTR (long terminal repeats) sequences are important for virus production. The modified THT promoter (TetO7-H1-TetA) binds TetR in a tetracycline dependent manner. Upon addition of doxycycline, this repression is relieved, allowing RNA polymerase III to transcribe the shRNA gene to induce RNAi [provided by Friederike Finsterbusch].

3.2.6 DNA damage

To induce DNA double strand breaks, HeLa-tetRA5 infected cells were seeded at a density of 0.3×10^6 cells in 35 mm tissue culture dishes. A double thymidine block was performed and cells irradiated with 8 Gy using a ^{137}Cäsium irradiation source 7 hours after release from the thymidine block, i.e., when they were in G2-phase. The first cell sample was taken directly after the second thymidine treatment (at the G1/S transition), a second 1 hour before γ-irradiation, and samples at 1, 3, 5, 7 and 17 hours after IR treatment. Cell were fixed in ethanol for analysis by flow cytometry or lysed in sample buffer for immunoblotting experiments.

3.3 "Western" blotting

3.3.1 Cell lysis

Cells were lysed by resuspending the cell pellet with RIPA (RadioImmuno-Precipitation Assay) buffer. To avoid protein degradation, all steps were carried out on ice or at 4 °C, respectively. The first step included harvesting of the cells through trypsination from a 35mm dish. For lysis, resuspended cells were incubated in 50 µL RIPA buffer on ice for 30 minutes, followed by centrifugation for 10 minutes at 16.100 rcf. The supernatant was removed, snap-frozen in liquid nitrogen and stored at –20 °C.

Alternatively, total cell extracts were performed by lysing 1×10^6 cells in 100 µL 1x SSB + 5% β-mercaptoethanol.

Protein samples were denatured at 95 °C for 10 min, spun down and sonicated to shear the DNA.

3.3.2 Bradford Assay

The protein concentration in the protein lysates was determined using the Bradford assay according to the manufacturer's manual for microtiter plates. BSA was used as protein-standard to obtain a calibration curve.

3.3.3 Sodium-dodecylsulfate polyacrylamide gel electrophoresis

To be able to detect proteins by immunoblotting, proteins were first separated by denaturing sodium-dodecylsulfate polyacrylamide gel-electrophoresis (SDS-PAGE). Gel preparation was carried out according to the protocol described in chapter 2. After polymerization of the separating gel, the components of the stacking gel were mixed and poured on top of the separating gel. Thereafter, the gel was placed in the electrophoresis-chamber, filled with SDS-PAGE running buffer. The cell lysate was mixed with 4x SSB + β-mercaptoethanol, boiled at 95 °C for 10 min, spun down and sonicated. Equal amounts of protein samples as well as a molecular weight standard were loaded and electrophoresis performed at 40 mA and 200 V with water cooling.

3.3.4 Immunoblotting

After completion of electrophoresis, the separated proteins were transferred to a nitrocellulose membrane using a semi-dry blotter. The gel was placed on a nitrocellulose membrane between 6 sheets of Whatman 3MM filter paper, which were soaked in 1x Transferbuffer. Air bubbles between the gel and the membrane were carefully removed and transfer was done for 1h 45 min (I = 0.8 mA/cm^2, constant). Transfer efficiency was assessed by incubation of the nitrocellulose membrane with Ponceau S staining for 5-10 minutes, followed by destaining in water.

To block non-specific binding sites, the membrane was incubated in membrane blocking buffer for 1 h at room temperature under agitation to prevent non-specific binding of the antibodies. Subsequently, the membrane was incubated with the primary antibody, diluted in membrane blocking buffer, overnight at 4 °C under agitation in a 50 mL tube. The next day, the membrane was washed thoroughly in washing buffer 3 times for 5 minutes under agitation to remove residual antibody. To visualise the bound primary antibodies, the membrane was

incubated with the secondary, HRP-conjugated antibody, diluted in membrane blocking buffer for 1 h at room temperature with agitation. The membrane was washed again in washing buffer 3 times for 5 minutes under agitation to remove residual secondary antibody with subsequent incubation in ECL reagent for 1 minute at room temperature. Excess of ECL was removed and the membrane exposed to Plus Medical X-ray (AGFA) and High performance chemiluminescence (GE Healthcare) films.

3.4 Cell synchronisation (DTB)

Cells grown under standard conditions proliferate asynchronously, i.e., they are in different phase of the cell division cycle. To facilitate the analysis of cell cycle phase specific events, cells have to be synchronised, e.g. by chemical methods, which employ cell cycle 'checkpoint' mechanisms to halt cell cycle progression at defined positions. After enrichment in this specific phase the chemical agent can be removed allowing the cohort of arrested cells to progress synchronously into the next steps in the division cycle. I used nocodazole treatment to block cells in mitosis as well as the so-called double thymidine block to block cells at the G1-S transition.

3.4.1 Nocodazole treatment

Nocodazole treated HeLa cells served as a positive control for flow cytometry as well as for immunofluorescence. HeLa cells were seeded in 10 cm dishes in culture medium and grown to 70 % confluency. After cells attached to the dish, cells were treated with 250 nM Nocodazole, a microtubule-depolymerization agent, for 4 hours. The detached mitotic cells were collected by a "shake-off", pelleted by centrifugation at 1300 rpm for 5 minutes at room temperature, washed in PBS and fixed in ethanol.

3.4.2 Double Thymidine Block

Cells were seeded in culture medium in 6-well tissue culture plates at a density of 0.3×10^6 per well. Six to 8 hours later thymidine diluted in culture medium was added to a final concentration of 2.5 mM for 16 hours. After the first block, cells were washed 2 times in PBS for 3 minutes each and fresh culture medium was added for 8 hours. Again, cells were treated with 2.5 mM thymidine diluted in culture medium for 16 hours. After the second block, cells were washed two more times in PBS for 3 minutes each and culture medium was added. The first sample, named 0 h release sample, was harvested by trypsination and fixed in ethanol for

analysis by flow cytometry. Further samples were harvested every 2 hours until 14 hours and care was taken to collect all cells.

3.5 Flow cytometry

Flow cytometry was used to determine cell size, granularity, their mitotic index and DNA-content, by measuring forward scatter (FSC), side scatter (SSC), fluorescence intensity in the FL1 channel (GFP, Alexa-488 visualized phospho-histone H3 signals), as well as propidium iodide fluorescence in the FL2 and FL3 channels, respectively.

For flow cytometry analysis, cells were fixed in ethanol, centrifuged in a microcentrifuge at 2000 rpm for 5 minutes at room temperature. The supernatant was removed and the pellet was resuspended in PBS and transferred into 'facs'-tubes. After pelleting at 1800 rpm for 5 minutes at 8 °C in a Sorvall RT7 Plus centrifuge the supernatant was decanted and the pellet resuspended in 0.25% Triton X-100 in PBS and incubated for 10 minutes at 4 °C to permeabilize the cells. After pelleting and washing, cells were incubated with the first antibody diluted in WB for 1 hour at room temperature. Subsequently, the cells were washed again with WB, pelleted, resuspended and incubated with the secondary fluorochrome-labelled antibody for 1 hour at room temperature in the dark. Next cells were washed again in WB and incubated with DNA staining solution, and analysed by flow cytometry.

To adjust the sensitivity settings of the flow cytometer, cells were also left unstained, or were only stained with one dye. Analysis of unlabelled and single labelled cells allowed the sensitivity adjustment of each detection channel as well as the compensation settings to avoid channel crosstalk.

The following figure should give an overview how flow cytometry data were analyzed using CellQuest Pro. Every single cell that passes the laser will be recorded with its data including cell size, internal complexity, as well as fluorescence signals of PI- and GFP/Alexa-488.
The primary gating (R1) was applied according to the FSC/SSC signals, which is represented by the dot plot on the upper left side. The x-axis represents the forward-scatter (FSC) values of the measured cells, which are plotted against the side scatter (SSC) values along the y-axis. Cells with too high or too low signals were excluded, because they might be due to cell clumps, hyperploid, or dead cells. Cells in R1 were then further analysed for fluorescence intensities. To be able to perform reliable DNA quantification, red fluorescence signals

correlated to the area and width of the cells were recorded in the FL3 channel to be able to discriminate multiplets (cell clumps) and single cells. Signals derived from individual cells were again gated (R3, in the lower left dot plot) and used to derive DNA histograms (upper right) as well as double fluorescence dot plots for determination of the mitotic index (lower right dot plot panel). The histogram represents the cell cycle phases according to their DNA-content. The x-axis displays the PI-fluorescence intensity and the y-axis shows the cell counts. The 4 indicated markers (M1-M4) indicate the different cell cycle phases. M1 indicates the G1-phase (1C = G1), M2 represents the S-phase (1C < S-phase < 2C), M3 shows cells in G2/M-phase (2C= G2/M) and M4 indicates the sub-G1-phase (dead cells). The last dot plot on the lower right side represents the PI signal on the x-axis against the FITC/Alexa-488 signal. This plot was used to discriminate cells that are in G2-phase and in M-phase, respectively. The data marked with a red rectangle were then transferred to a Microsoft Office Excel spreadsheet for quantitative analysis.
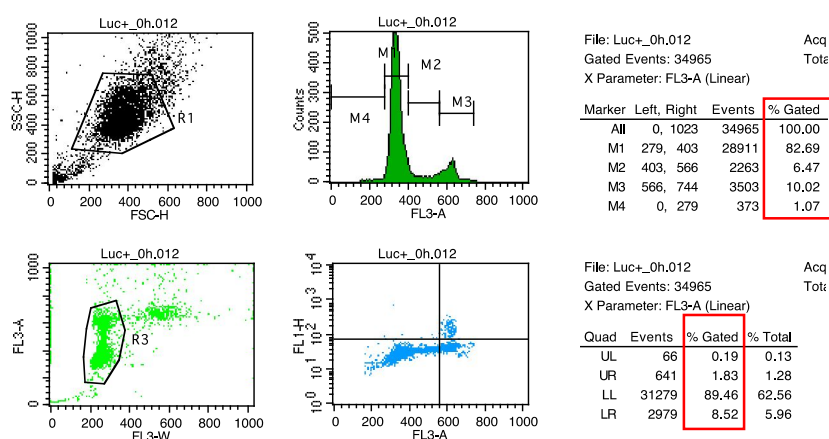

Figure 12: Summary of flow cytometry data analysis. Labelled cells were recorded on a BD FACScan flow cytometer and data analyzed by CellQuest Pro. Settings were adjusted according to the controls performed in each experiment. A representative analysis flow for determination of the cell cycle profile as well as mitotic index of untreated HeLa cells is shown.

3.6 Immunofluorescence microscopy

Immunofluorescence microscopy was used to establish a protocol for determining the mitotic index by staining for the mitosis specific phosphorylation of histone H3 on serine 10. Because I also wanted to simultaneously determine the cell cycle distribution by DNA staining, I used an alcohol based cell fixation protocol, which is known to work best for DNA content quantification by flow cytometry. For immunofluorescence experiments nuclear counterstaining was performed with 1µg/mL Hoechst 33342. Phospho-Ser10 on histone H3 was detected by direct as well as indirect immunofluorescence technology.

3.6.1 Direct Immunofluorescence

For direct immunofluorescence experiments fixed cells were centrifuged at 2000 rpm for 5 minutes at room temperature. The supernatant was removed and the pellet was resuspended in PBS. After pelleting at 1800 rpm for 5 minutes the supernatant was decanted and the pellet was resuspended in PBS supplemented with 0.25% Triton X-100 and incubated for 10 minutes at 4 °C to permeabilize the cells. After pelleting and washing in 'washing buffer for flow cytometry (WB)', cells were incubated in the dark with FITC-conjugated phospho Histone H3 antibody diluted in WB for 1 hour at room temperature. Subsequently, the cells were washed again with WB and incubated for 10 minutes at room temperature in the dark with Hoechst 33342 (1 µg/mL in WB) for nuclear counterstaining. Next, cells were washed again in WB, resuspended in PBS and placed on glass-bottom dishes for analysis on an inverted fluorescence microscope.

3.6.2 Indirect Immunofluorescence

Fixed cells were centrifuged at 2000 rpm for 5 minutes at room temperature. The supernatant was removed and the pellet was resuspended in PBS. After pelleting at 1800 rpm for 5 minutes the supernatant was decanted and the pellet was resuspended in PBS supplemented with 0.25% Triton X-100 and incubated for 10 minutes at 4 °C. After pelleting and washing in WB, cells were incubated with the first antibody (e.g. rabbit anti phospho-Histone H3) diluted in WB for 1 hour at room temperature. Subsequently, the cells were washed with WB and the pellet resuspended in WB containing the secondary, fluorochrome-labelled antibody for 1 hour at room temperature in the dark. Hoechst 33342 was added to the samples to a final concentration of 1 µg/mL diluted in WB for 10 minutes, before cells were washed once in WB, resuspended in PBS and finally transferred to glass-bottom dishes for microscopy.

3.7 Microscopy and live cell imaging

Microscopy was performed on an inverted automated epifluorescence ZEISS Axiovert *200M,* controlled by *Metamorph* software (Universal Imaging, Inc.) version 7.0. For epifluorescence microscopy a 100W mercury vapour lamp (350-650nm from Osram, HBO103W-2) was used in combination with appropriate filter units. Attached to the base port of the microscope was a highly sensitive, 12bit, cooled Collsnap*fx* camera with a resolution of 1300x1030 6.7 µm x 6.7 µm pixels. For live cell imaging, the microscope was additionally equipped with a CO_2 incubator (CTI 3700) and a heating plate (tempcontrol 37-2). The *Metamorph* software

enabled functional control of the microscope (e.g. acquisition of time-lapse movies, image analysis, overlays and quantitative analysis). Light source for phase-contrast microscopy was a 100W halogen lamp, controlled by the light manager – a fully automatic light controlling device featuring automatic setting of previously selected brightness levels and contrast options for each of the six objectives, positioned on the objective revolver (10x, 32x, 40x, 40x oil, 63x oil and 100x oil).

4 Results and Discussion

4.1 Transfection of HEK 293T

For production of infectious lentiviral particles, I used human embryonic kidney (HEK) 293 T cells, because they are easy to transfect and are known to yield high levels of lentiviral particles.

HEK 293T cells were grown in 6-well plates and transfected with lentiviral plasmids together with the packaging plasmid psPAX2 and pVSV-G for viral pseudotyping. When I used the TetR-GFP fusion protein expression vectors, I could monitor the transfection efficiency by fluorescence microscopy of living cells as shown in Figure 13.
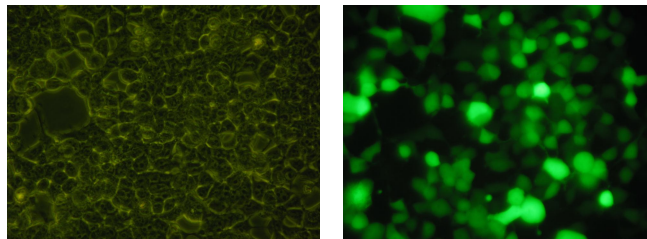
Figure 13: Transfection of HEK 293T with Lucsh-tetR-GFP construct. HEK293T cells were transfected with pHR-THTIII-Luciferase_shRNA-tetR-GFP, pSPAX2 and pVSV-G. 48 hours after transfection GFP expression was monitored by live cell fluorescence microscopy. As can be seen in the right image, the majority of cells expresses GFP protein.

Lipofection-based transfection of the lentiviral plasmids turned out to be very effective (transfection efficiencies were ways greater than 50%) and did, therefore not require any further optimisation.

4.2 Establishment of conditional RNAi cell lines

4.2.1 Transduction of HeLa-tetRA5 cells

To generate stable conditional RNAi cell lines I transduced HeLa-tetRA5 cells, which stably express humanized TetR, with lentiviral particles encoding for caspase 2 and Luciferase specific shRNA expression vectors. Transduction was achieved by incubating HeLa cells with filtered HEK 293T media supernatants obtained 48 and 72 hours after transfection with plasmid vectors for lentivirus production as described above. Cells were incubated for 3 days

and then expanded to 10 cm dish in the presence of 2.5 µg/ml puromycin for selection of stable integrants. For all downstream applications I worked with the bulk cell line, i.e. with all cells that survived the puromycin selection protocol.

4.3 Characterization of conditional Caspase 2 RNAi cell lines

4.3.1 HeLa-tetRA5 derived lines

HeLa-tetR-A5-Casp2-1sh-puro, HeLa-tetRA5-Casp2-3sh-puro and HeLa-tetRA5-Lucsh-puro cells were seeded in 6 well plates at a density of 0.4 or 0.2 x 10^6 cells, treated with 500 ng/mL doxycycline and grown for up to 5 days. Cells were harvested by trypsination at indicated time-points, pelleted, and resuspended in 1x SSB supplemented with 5% β-ME. Equal amounts of protein were separated by 12% SDS-PAGE and caspase 2 expression levels evaluated by immunoblotting.
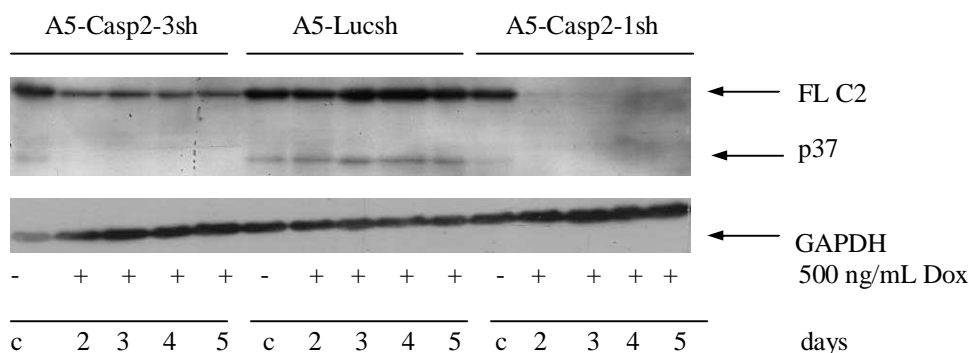
Figure 14: Characterization of the doxycycline-induced down-regulation of Caspase2 expression level in HeLa-tetR-A5 infected cell lines. I seeded 0.4 x 10^6 cells for the 48 hour and 72 hour samples and 0.2 x 10^6 for the 96 hour and 120 hour samples, respectively. Doxycycline untreated cells (c) showed a strong caspase 2 signal. Blots were reprobed with anti-GAPDH antibody to evaluate proper loading. Full length (FL) caspase 2 and its autocleavage product p37 were detected with a monoclonal anti-Casp2 antibody.

As shown in Figure 14, doxycycline administration led to a noticeable decrease in caspase 2 expression in A5-Casp2-1sh cells but only modestly affect the caspase 2 expression levels in A5-Casp2-3sh cells. Luciferase shRNA expression in the presence of doxycycline had no influence on caspase 2 protein level confirmed by a strong band at 53 kDa. Moreover, doxycycline treatment had no adverse effect on cell proliferation and Hela-tetRA5 infected cell lines could be permanently grown in 500 ng/mL doxycycline.

4.3.2 HeLa-tetR-GFP cell lines

HeLa-Casp2-3sh-tetR-GFP and HeLa-Casp2-1sh-tetR-GFP cells, which were generated by the technician Veronika Rauch and already available at the beginning of my master work, were seeded in culture medium in 6 well plates at a density of 0.4 x 10^6 cells. To determine the optimal doxycycline concentration required to induce efficient knockdown of caspase 2, cells were first incubated with different concentrations of doxycycline. 24 hours after induction, cells were harvested and the final pellets were resuspended in 1x SSB / 5 % β-ME. Equal amounts of protein were separated on a 12 % SDS polyacrylamide gel, and subjected to immunoblotting using antibodies specific for caspase 2 as well as for GAPDH as loading control.
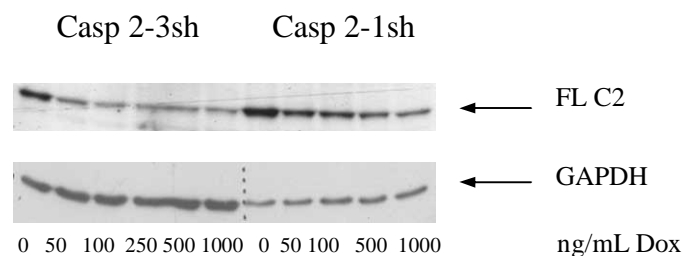
Figure 15: Down-regulation of caspase 2 expression by RNAi in HeLa-tetR-GFP cells. Transgenic HeLa cells were incubated with increasing concentrations of doxycycline to induce the expression of the shRNA. 24h after induction, cells were harvested and processed for immunodetection of the target protein as well as for a house keeping protein as a protein gel loading control. The RNAi effect is more efficient in Casp2-3sh cells, because there is a significant decrease of caspase 2. Full length (FL) caspase 2 was detected with the rat-anti-Casp2-11B4 antibody as a band of 53 kDa.

As can be seen Figure 15, the Casp2-3sh cell line showed a more efficient knock-down but the effect was less dose-dependent than in the Casp-2-1sh cell line. Because no adverse effect on cell proliferation or survival could be detected when incubating control HeLa cells with up to 1 µg/mL doxycycline, I used 500 ng/mL for Casp2-3sh cell line and 1 µg/ml doxycycline for Casp2-1sh cell line for all further induction experiments. To determine the optimal time point for experiments in knockdown cells, I next performed a time course experiment.

HeLa-Casp2-3sh-tetR-GFP and HeLa-Casp2-1sh-tetR-GFP cells were seeded in 6 well plates at a density of 0.4 or 0.2 or 0.1 x 10^6 cells. The culture medium supplemented with doxycycline was exchanged every 2 days because doxycycline is known to be unstable at 37°C. As indicated in Figure 16, cells were harvested every 24 hours for preparation of whole cell lysates and determination of caspase 2 expression levels by immunoblotting. As can be seen in Figure 16, doxycycline-induced decrease in caspase 2 expression can be detected already after 24 hours but minimum levels are only seen at day 4.
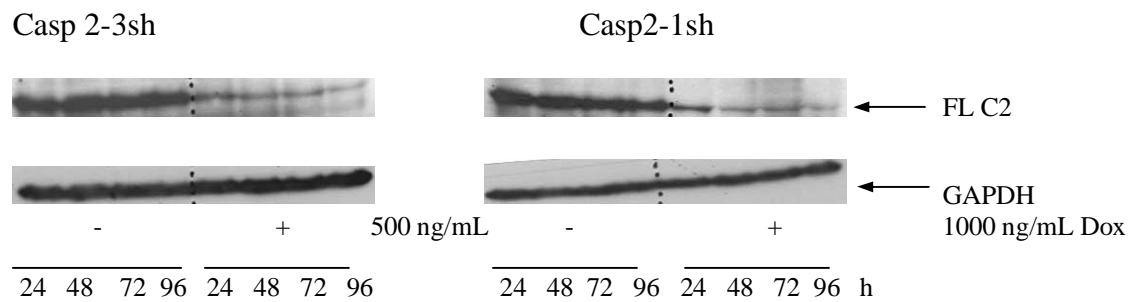
Casp 2-3sh   Casp2-1sh

-        +   500 ng/mL   -   +   1000 ng/mL Dox

24 48 72 96 24 48 72 96   24 48 72 96 24 48 72 96 h

Figure 16: Time course of the effect of doxycycline treatment on caspase 2 expression. I seeded 0.4 x 10^6 cells for the 24 hour sample, 0.2 x 10^6 for the 48 hour and 72 hour samples and 0.1 x 10^6 cells for the 96 hour sample, respectively to guarantee unrestricted cell proliferation. Cells were cultured in culture medium supplemented with 500 ng/mL and 1000 ng/mL doxycycline, respectively. At indicated time-points, cells were harvested by trypsination, washed once in PBS and lysed in 1x SSB and further separated on a 12% SDS polyacrylamide gel. Protein samples were again probed with rat-anti-Casp2 11B4 antibody.

4.4 Determination of mitotic cells with α-phospho-histone H3 antibody by fluorescence microscopy

In my thesis, I wanted to test the role of caspase 2 in the DNA damage G2/M checkpoint response that controls entry into mitosis. According to a hypothesis put forward in the recent literature [17], cells lacking caspase 2 should have a weaker G2/M checkpoint and fail to prevent entry into mitosis after DNA damage. To be able to test this hypothesis, I had to establish a protocol for detection of mitotic cells by fluorescence microscopy as well as flow cytometry. Although both techniques are based on the detection of fluorescence signals, the protocols are not always fully compatible due to the employed fluorochromes and available detection channels. I decided to use detection of mitotic cells by immunostaining for phosphorylated histone H3 (Ser10), a mitosis specific marker, using dyes compatible with standard propidium iodide DNA staining for flow cytometry.

4.4.1 HeLa and HeLa-tetR-GFP cell lines

HeLa-Casp2-3sh-tetR-GFP cells were harvested and fixed in ethanol for direct immunofluorescence experiments to detect mitotic cells by a FITC-conjugated anti-phospho-histone H3 antibody. As a nuclear counterstain, I used Hoechst 33342. Experience from previous experiments suggested that the GFP protein efficiently leaks out of cells fixed by ethanol treatment. To test whether GFP depletion is complete, I stained asynchronously growing cells with the DNA dye Hoechst 33342 and recorded fluorescence levels in the 'blue' as well as the 'green' channel. I used Hoechst 33342, because there is no significant leakage of the 'blue signal' into the 'green' channel.
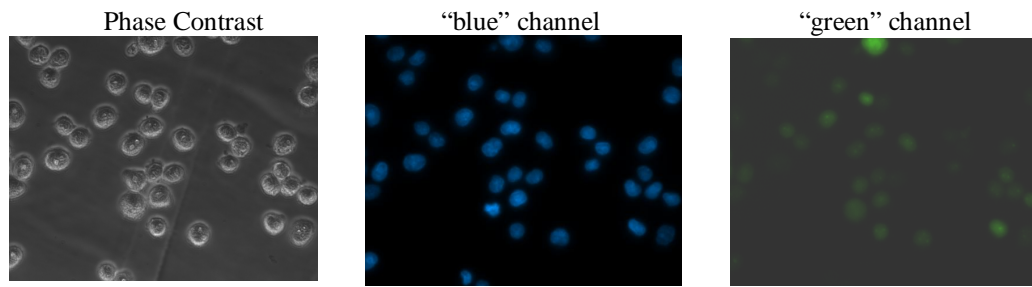
Figure 17: HeLa-Casp2-3sh-tetR-GFP cell line stained with Hoechst 33342. HeLa cells were fixed in ethanol overnight at -20 °C and incubated with 1 μg/mL Hoechst for 10 minutes in glass bottom culture dishes. Imaging was performed on a ZEISS Axiovert *200M* microscope with a 40x objective.

Figure 17 shows asynchronously grown HeLa-Caspase2-3sh-tetR-GFP cells stained with Hoechst 33342. As can be seen in the rightmost image, a rather strong signal could be detected in the 'green fluorescence' channel. Because this signal could not be detected in non-transgenic HeLa cells, I excluded that this signal is due to cellular autofluorescence and must be due to residual GFP levels. Because this unexpected green fluorescence background signal might interfere with direct immunofluorescence using FITC-labelled antibodies I next tested other fluorochromes (Alexa546- and Alexa647-labelled secondary antibodies) in combination with FITC labelled antibodies.
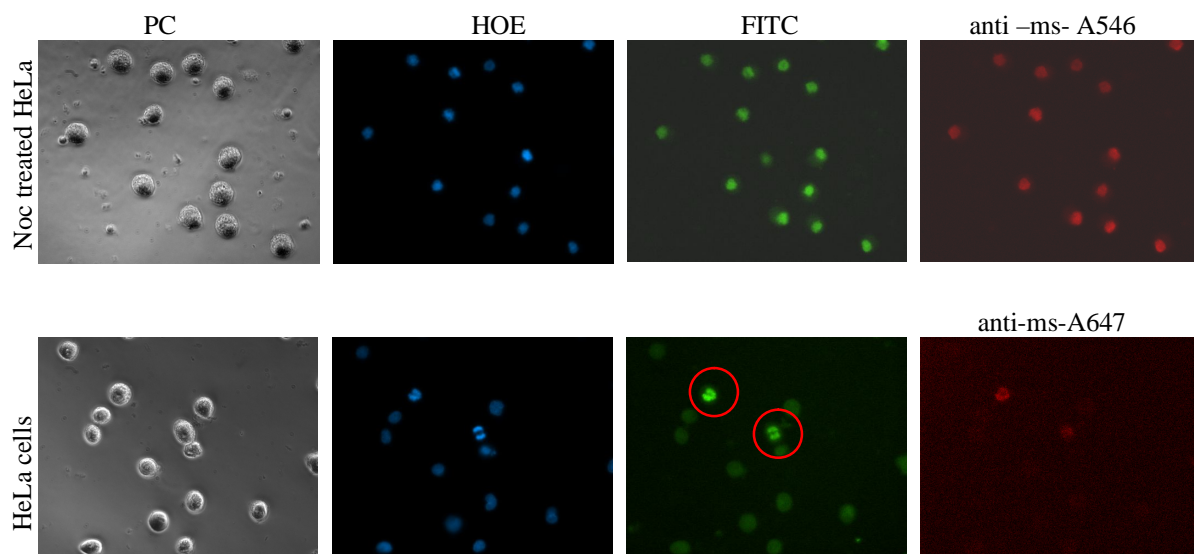

Figure 18: Direct and indirect immunofluorescence for detection of phospho-histone H3 in mitotic HeLa cells. First row: Nocodazole treated HeLa cells were collected by a "shake-off", fixed in ethanol and stained with Hoechst, FITC-conjugated antibody targeting phospho-histone H3 and Alexa546-labelled secondary antibody. Second row: To verify the specific binding of the antibody targeting phospho-histone H3 to mitotic cells only, I used asynchronously grown HeLa cells, fixed in ethanol and stained as above. As indicated by the red circles, only cells in mitosis give a bright signal. In contrast to the indirect fluorescence protocol, the directly labelled antibody gives some background also in non-mitotic cells, suggesting that an indirect staining procedure might be more reliable. All pictures were taken at 40-fold magnification and with the same exposure time.

Nocodazole treated, mitotically arrested HeLa cells were fixed in ethanol and incubated first with FITC-labelled mouse-anti-phospho-histone H3 antibodies, followed by an incubation

with anti-ms-Alexa546-labelled secondary antibody. Finally, cells were also stained with Hoechst 33342 to stain the nuclei. As can be seen in Figure 18, all nocodazole treated cells (top row) stained brightly for phospho-histone H3. As expected, only mitotic cells (circled cells in the bottom row) but not interphase cells stained brightly with this antibody.

4.4.2 HeLa-tetRA5 infected cell lines

To detect mitotic cells in HeLa-tetRA5-Casp2-3sh-puro and HeLa-tetRA5-Casp2-1sh-puro cell lines, cells were fixed in ethanol and incubated with anti-phospho-histone H3 antibodies, followed by Alexa488-conjugated secondary antibodies as well as Hoechst 33342.
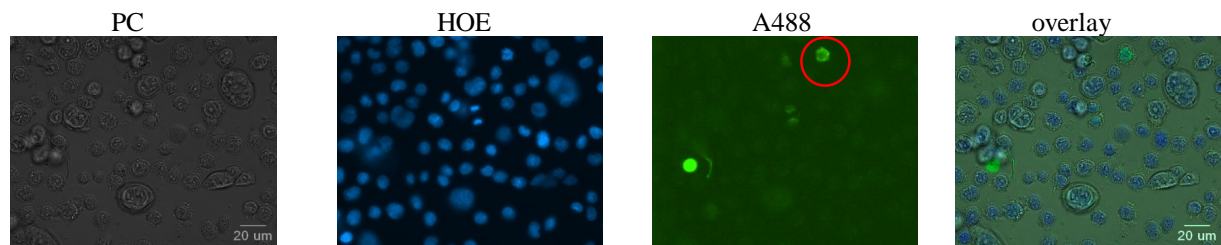
Figure 19: Detection of mitotic cells by indirect immunofluorescence technology targeting phospho-histone H3 in HeLa-tetRA5-Caspase2-1sh-puro cells. Cells were harvested by trypsination, fixed in ethanol and stained with Hoechst 33342, phospho-histone H3 antibody and A488-conjugated secondary antibody. The red circle indicates a cell in prophase.

As shown in Figure 19, the brightest signals correspond to mitotic cells (circled). Interphase cells, however, display only low green background fluorescence.

4.5 Cell cycle analysis

The analysis of the DNA damage checkpoint can be performed by biochemical means, e.g. by detecting changes in protein levels that are known to be involved in checkpoint regulation, by proteins known to control the cell division cycle as well as by cell biological methods able to monitor entry into mitosis. A common prerequisite for these analyses is that cells to be analysed should be synchronised in their state of the cell cycle. I therefore tested the double thymidine block (DTB) protocol as a chemical synchronisation method. Thymidine is rapidly taken up by cells and converted into dTTP, which- at high doses – is an allosteric inhibitor of ribonucleotide reductase, which is responsible for converting ribonucleotides into deoxyribonucleotides. Thus, high doses of thymidine deplete cells from dCTP, which is required for DNA replication. During the first exposure to high levels of thymidine DNA replication is blocked and cell cycle progression halted. Upon release, cells proceed in their

cell cycle before they are again exposed to thymidine, which now causes all cells to arrest at the onset of S-phase. Upon washing out the excess thymidine, cells are now able to progress in a synchronous manner throughout the remaining phases of the cell division cycle.

First, I tested whether mouse embryonic fibroblasts (MEFs) can be synchronised using a DTB, established a protocol for synchronising HeLa cells and then employed phospho-histone H3 staining to determine the mitotic index.

4.5.1 Synchronisation of immortalized MEFs & MEFs C2^{-/-}

A DTB was also employed for cell cycle synchronisation experiments using immortalized control as well as caspase 2 knock-out MEFs. Cells were seeded in 6 well plates at a density of 0.15 x 10^6 cells and after the second thymidine block cells were harvested at the time points indicated in Figure 20 by trypsination, fixed in 70 % ethanol and prepared for DNA content analysis by flow cytometry.
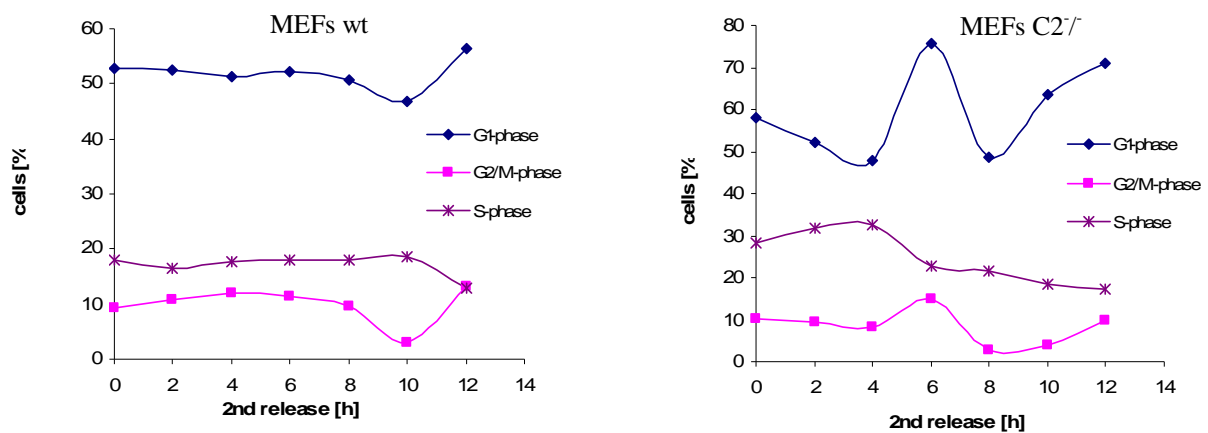

Figure 20: Cell cycle analysis of MEFs wt and MEF C2^{-/-} after DTB. The DTB did not work in MEFs wt cells and led to a G1 arrest. However, caspase 2 knock-out MEF lines could be synchronized.

As can be extracted from the data summarised in Figure 20, wild-type MEFs could not be synchronized by employing a DTB protocol, because cells appear to arrest in G1-phase. In contrast, a fraction of caspase 2 knock-out MEFs could be synchronized, as indicated by an increase in cells in G2/M-phase (6 hours after the second thymidine block). This fraction appeared to be too small to be useful for biochemical analyses. I therefore continued to use HeLa RNAi cell lines for further analysis.

4.5.2 Synchronisation of HeLa-tetRA5-derived RNAi cell lines

HeLa-tetRA5-Casp2-1sh-puro and HeLa-tetRA5-Lucsh-puro cells were seeded in 6 well plates at a density of 0.3×10^6 and cultivated in the presence (+) or absence (-) of doxycycline. After the second thymidine block, cells were imaged by phase contrast microscopy every 2 hours, harvested, fixed and stored at -20 °C until further processing and analyses for DNA content by flow cytometry.
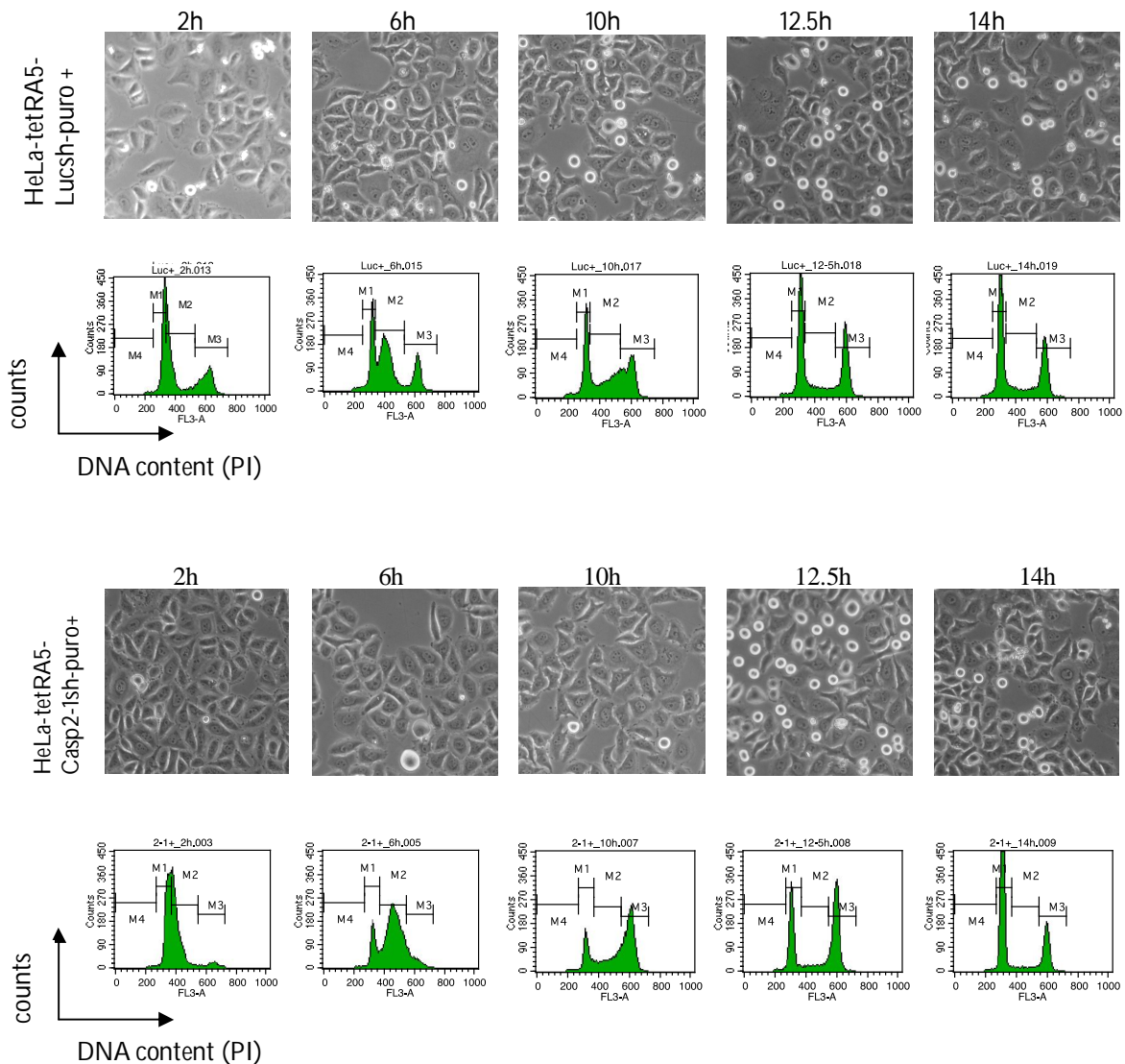

Figure 21: Phase contrast microscopy and DNA content analysis of HeLa-tetRA5-Lucsh-puro and induced HeLa-tetRA5-Casp2-1sh-puro cells. Samples were taken beginning at the indicated time points after release from the second thymidine block. Images were taken on a ZEISS Axio Observer A1 using a 10x objective.

As shown in Figure 21, induced caspase 2 RNAi cells were found to be better synchronised than control induced Luciferase RNAi cells. This is evident by the absence of the G2/M peak in the caspase 2 RNAi cells. In contrast, however, caspase 2 RNAi cells appeared to enter S-

phase faster than controls after release from the second thymidine block. This phenomenon could be explained by the fact that caspase 2 has recently been implicated in the regulation of p21CIP levels, a key regulator of the G1/S checkpoint [23]. Control Luciferase RNAi cells, in contrast, arrest at the G1/S boundary as well as before entry into mitosis. Progression through the cell division cycle was also more synchronous in caspase 2 RNAi than in control cells. This was evident in the phase contrast images, i.e. a higher fraction of rounded up mitotic cells are seen around 12.5 hours after the release from the thymidine block. This better synchrony was also observable in DNA FACS analysis as shown in the DNA histograms in Figure 21.

In summary, these data show that both cell lines can be synchronized effectively using a DTB. The caspase 2 RNAi cell line seems to re-enter S-phase faster than the control cell line and fails to arrest at the G2/M transition in response to thymidine exposure. This suggests a difference in checkpoint responses in the two cell lines. Alternatively, the presence of the G2/M peak in the controls could be due to a fraction of cells that could not be synchronised by the double thymidine block.

4.6 Determination of the mitotic index

To be able to determine the mitotic index, I used the above described protocol for simultaneous detection of DNA content as well as the mitotic state of single cells.

First, I used HeLa-tetR-GFP RNAi cell lines. Cells were seeded in 6 well plates at a density of 0.15×10^6 cells. After the DTB, cells were harvested by trypsination, pelleted, washed once in PBS, fixed in 70 % ethanol and stored at -20 °C. For cell cycle analysis, cells were stained with PI as described in the Methods section. Figure 22 shows HeLa-Casp2-3sh tetR-GFP cells stained with PI only. After setting the R3 gate in the FL3 channel, cells were analysed in the FL1 (green) as well as FL3 channel. As can be seen in the corresponding dot plot, there is some signal in the FL1 channel that could be caused by autofluorescence and/or residual GFP levels.
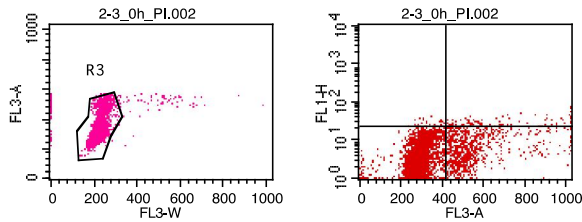
Figure 22: HeLa-tetR-GFP-Casp2-3sh cells stained with propidium iodide. The left panel shows the FL3 area vs. width dot plot to identify single cells. The right panel shows a dot plot of FL3 signals vs. FL1 signals. The signals in the FL1 channel are either due to green autofluorescence or residual GFP levels.

Because the green fluorescent background signal might have been caused by residual GFP levels, I then continued to use the HeLa-tetR cell lines for all further experiments. DTB synchronized cells were fixed, stained with propidium iodide and Alexa488-vizualized anti-phospho-histone H3 (Ser10) antibody and analysed by flow cytometry. Events were first gated on FSC vs. SSC values and FL3 vs. FL1 dot plots further analyzed.
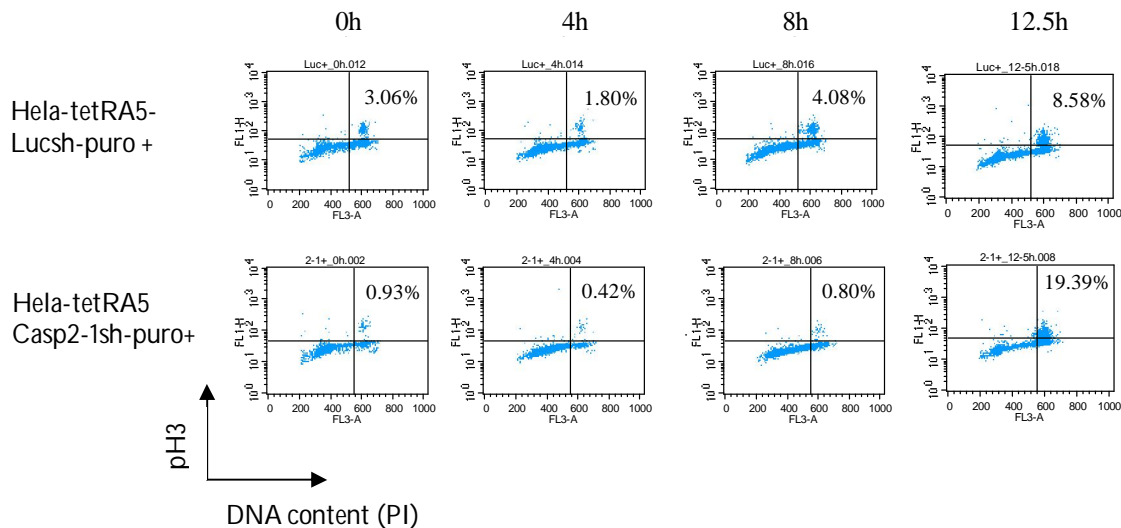

Figure 23: Representative dot plots of cells released from a DTB analyzed for DNA content (PI) and mitosis (pH3 staining). Cells were harvested after the second G1/S block every 2 hours up to 14 hours but just data at indicated time-points are presented.

As shown in Figure 23, control Luciferase RNAi cells still contain about 3 % mitotic cells at the end of the second thymidine block. Thus, these cells contain a fraction that could not be blocked at the G1/S transition and/or S-phase, which is most likely due to clonal heterogeneity of the cell line. Caspase 2 RNAi cell lines, however, contained only few mitotic cells at the end of the second thymidine block, consistent with the DNA content analysis shown in the histograms above.

Consistent with data presented in histograms, the mitotic index of A5-Casp2-1sh-puro+ cells reaches a maximum of 19.39 % after 12.5 hours in the second release period as compared with 8.58 % in control cells.
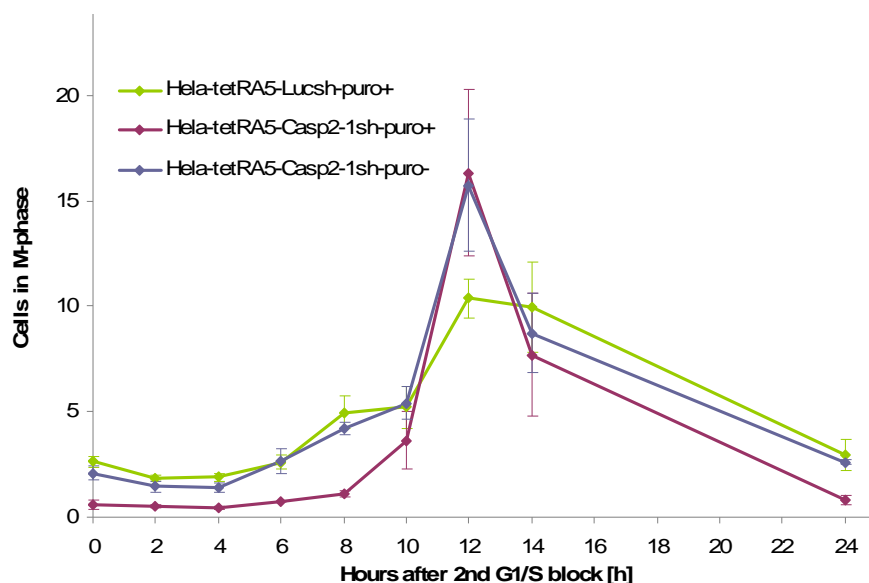
Figure 24: **Performance of the mitotic index upon a DTB.** Cells were synchronized by a double thymidine block, harvested by trypsination, stained with PI and phospho-histone H3 antibody for DNA content analysis and determination of the mitotic index by flow cytometry. The mitotic index shown is the mean of 3 independent experiments (mean ± SEM).

HeLa-tetRA5 RNAi cells were synchronized according to the DTB protocol and Figure 24 summarizes the mitotic indexes over time after release from a DTB. The induced caspase 2 RNAi cell line, indicated by the purple line, shows a more effective synchronisation than the controls. Caspase 2 knock-down leads to a maximum of mitotic cells 12 hours after release of the thymidine block in contrast to induced Luciferase RNAi and non-induced caspase 2 RNAi cell lines, which already show an increase in mitotic cells after 6 hours. Furthermore, Figure 24 reveals that both controls, HeLa-tetRA5-Luciferase cells and non-induced caspase 2 RNAi cells, react to the DTB in the same way, depicted by the green and blue line. Thus, the difference seen in the cell cycle parameters is not due to a clonal variance but due to the levels of caspase 2 present in the different cell lines. In addition, progression through mitosis also does not seem to be altered in RNAi cells as cells lose their phospho-histone H3 signals as rapidly as the control cell lines. In summary, depletion of caspase 2 seems to abrogate the small peak of mitotic cells seen around 8 hours after release from the DTB. This small peak of mitotic cells can be caused by cells that failed to become arrested in response to the DTB protocol or by cells that became arrested in G2 phase. Although further experiments are required to explain the nature of this 8h mitotic peak, the data suggest that caspase 2 levels affect cell cycle synchronisation efficiency.

In DTB synchronised cells as well as in irradiated cells, knockdown of caspase 2 did not seem to abrogate the G2/M checkpoint. This checkpoint is, however, tightly controlled and mainly operates by controlling the activity of CDK1 by phosphorylation on tyrosine 15. Any perturbance of this pathway has serious and deleterious consequences on cell cycle progression and cellular survival, because disruption of this checkpoint causes mitotic catastrophe. I conclude from my experiments that caspase 2 plays no essential function in this checkpoint.

4.7 Effect of DNA damage on the mitotic index

To determine whether caspase 2 affects the G2/M checkpoint in cells subjected to DNA damage, HeLa-tetRA5 caspase 2 RNAi as well as control Luciferase RNAi cell lines were synchronised by a DTB, left untreated or were irradiated with 8 Gy in G2-phase, i.e. 7 hours after the second block. Samples were taken immediately after the release, as well as 1, 3, 5, 7 and 17 hours after the IR-treatment and prepared for flow cytometry analysis which includes PI- and Alexa488-staining.
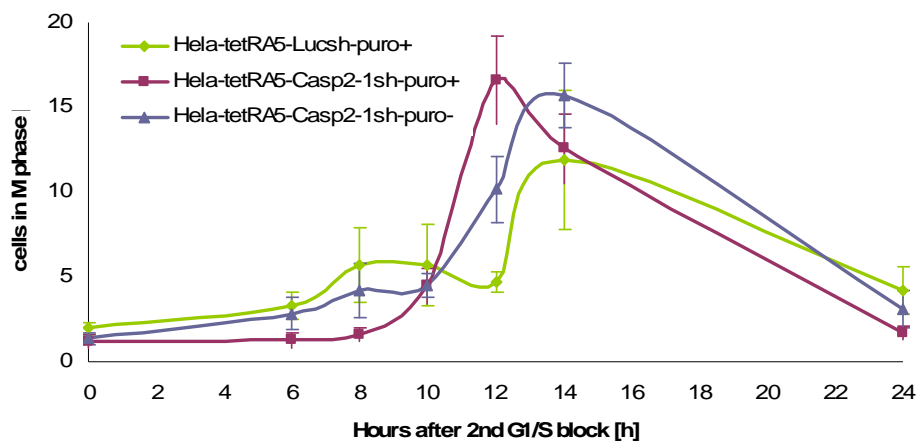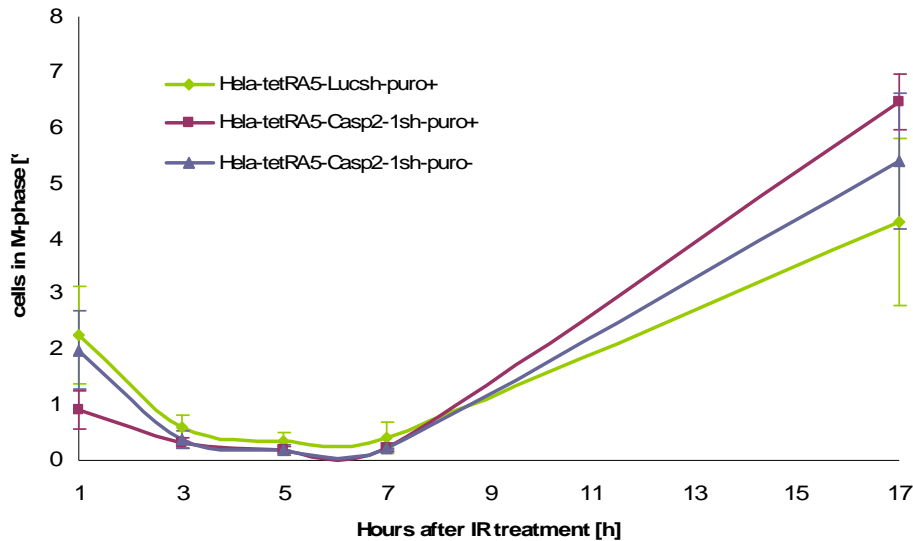
Figure 25: Comparison of the mitotic index in IR-untreated and IR-treated HeLa-tetRA5 RNAi cell lines.
To explore the influence of caspase 2 on the G2/M checkpoint, cells were synchronized by a double thymidine block and 7 hours after the second G1/S block treated with γ-radiation (8 Gy) to induce DNA damage. Cells were harvested 1, 3, 5, 7 and 17 hours after IR-treatment, stained for DNA content and phospho-histone H3 and analyzed by flow cytometry. The top graph shows the percentage of phospho-histone H3 positive cells in non-irradiated cells with the blue and purple lines representing uninduced and induced caspase 2 RNAi cells, respectively. The green line represents induced Luciferase RNAi cells.
The bottom graph shows phospho-histone H3 positive mitotic cells after IR treatment (mean ± SEM).

Figure 25 (upper diagram) shows the mitotic index of induced control Luciferase and caspase 2 RNAi cell lines as well as non-induced caspase 2 RNAi cells, released from a DTB. As already described above, the induced caspase 2 RNAi cell line was nicely synchronized and cells entered mitosis around 12 hours after the release from the DTB. In contrast, the non-induced cells, as well as the control Luciferase RNAi cells, showed a small peak of mitotic cells already at 8 hours after the release, while the majority of mitotic cells was seen to enter mitosis 14 h after the release from the DTB.
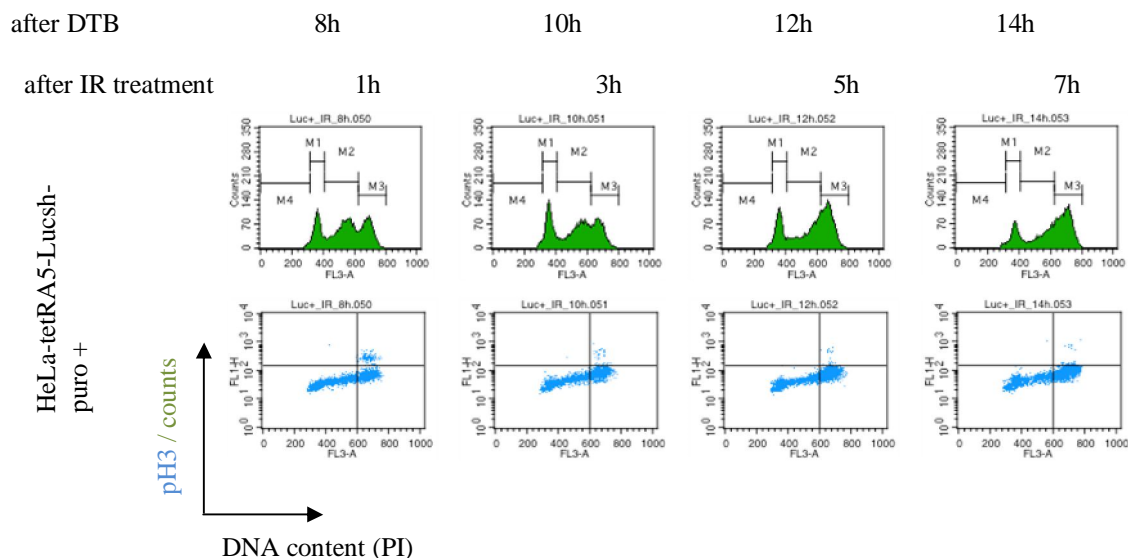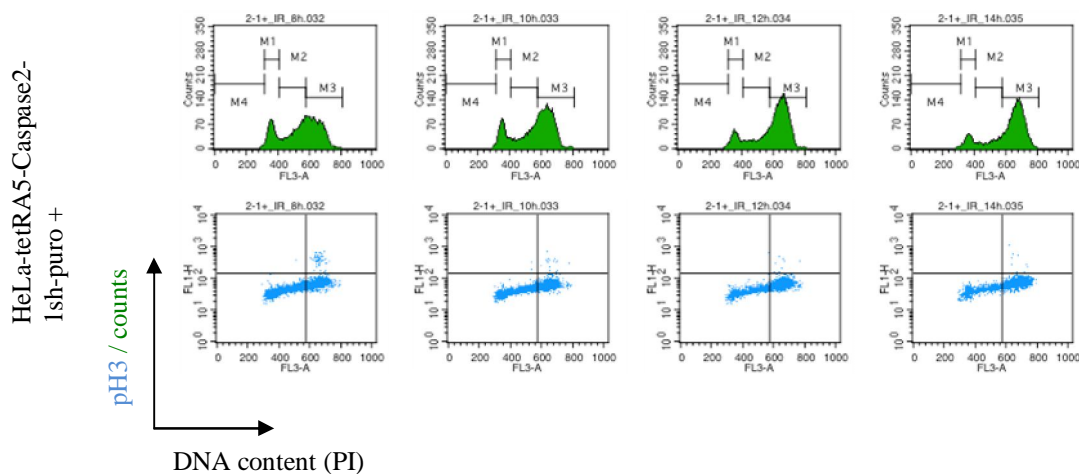
Figure 26: Dot plots and DNA content analysis of HeLa-tetRA5-Lucsh-puro and induced HeLa-tetRA5-Casp2-1sh-puro cells after IR-treatment following a DTB. Cells were DTB synchronized and irradiated 7 hours after the release from the second thymidine block. Cells were harvested 1 (8h after the second thymidine block), 3 (10h), 5 (12h) and 7 hours (14h) after the IR-treatment. The number of mitotic cells, depicted in the upper right quadrant of the FL1 vs. FL3 plots, declined over time (bottom row) because they became arrested at the G2/M transition as can be seen in the DNA histograms (top row).

As can be seen in Figure 26 control Luciferase RNAi cells treated with 8 Gy of ionizing radiation at 7 hours after the release from the DTB arrested in G2-phase and the number of mitotic cells declined, consistent with a functional G2/M checkpoint in control cells.

Interestingly induced caspase 2 RNAi cells also appeared to arrest in G2-phase, suggesting that caspase 2 is not required for the G2/M checkpoint in response to γ-irradiation in HeLa cells. This result is not consistent with the hypothesis that loss of caspase 2 results in an abrogation of the G2/M checkpoint due to DNA damage, which would result in an earlier entry into mitosis.

To verify the induction of a DNA damage response after irradiation, phospho-H2A.X (Ser 139) levels, which is phosphorylated by ATM and ATR in response to DNA damage, were evaluated by immunoblotting. As can bee seen in Figure 27, phospho-H2A.X signals were readily detectable in induced and irradiated caspase 2 as well as Luciferase RNAi cells, demonstrating that γ-irradiation was effective in both cell lines.
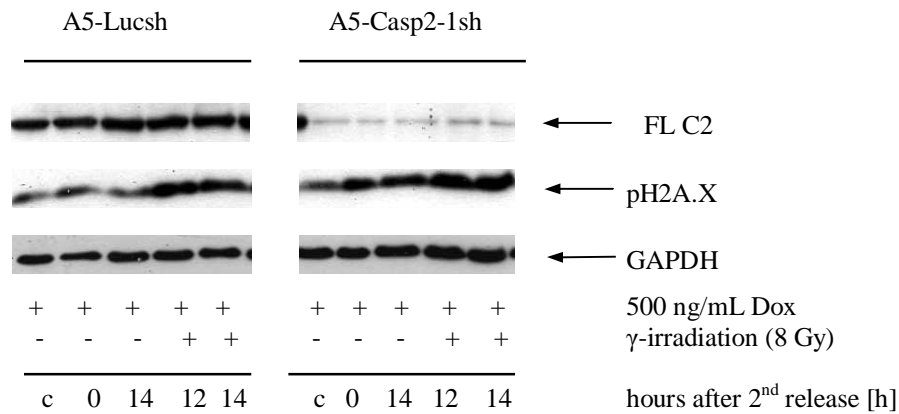
Figure 27: **Determination of DNA damage induction following IR-treatment.** After a DTB with subsequent IR- treatment after 7 hours, cells were harvested at indicated time points and whole cell lysates were prepared. Caspase 2 expression levels as well as phospho-H2A.X levels, which is a marker for DNA double strand breaks, were evaluated. As shown in the Figure, IR-treatment led to a marked increase in phosphorylated histone H2A.X that indicates additional DNA damage.

The above results showed that caspase 2 RNAi cells arrested efficiently at the G2/M transition after ionizing radiation. Inspection of the cell cycle phase distribution data, however, revealed that control cells transiently accumulated in G1 phase after irradiation, while induced caspase 2 RNAi cells did not (see Figure 28 lower panel), indicated by a purple line. The reason for this transient rise is unclear at the moment but could be owing to differences in cell cycle progression in these different cell lines. However, caspase 2 deficient cells showed an increase of cells in G1-phase following IR treatment in contrast to controls, depicted in Figure 28 (lower panel). As shown above, control cells (Luciferase RNAi as well as non-induced caspase 2 RNAi cells) contained a fraction of cells that already entered mitosis around 8 hours after release from the DTB. Thus, these cells might have escaped DNA-damage induced G2 arrest and progressed through mitosis into G1-phase. Because HeLa cells lack functional p53, the G1-DNA damage checkpoint is likely to be impaired and cells would continue with cell cycle progression.

The upper panel in Figure 28 illustrates cells in G1-phase after release from the DTB without IR treatment. In contrast to the controls, induced caspase 2 RNAi cells show a stronger decrease of cells in G1-phase until 12 hours before increasing again in G1-phase, which is in line with our observation, that induced caspase 2 RNAi cells reaches a maximum of mitotic cells 12 hours after release from the DTB, which is depicted in Figure 25 (upper panel). Control cells, however, show a growing number of cells in G1-phase starting 8 hours after the second G1/S block, which could be explained by the fact that cells already stay in mitosis at 8 hours after the release from the DTB (see Figure 25 upper panel).
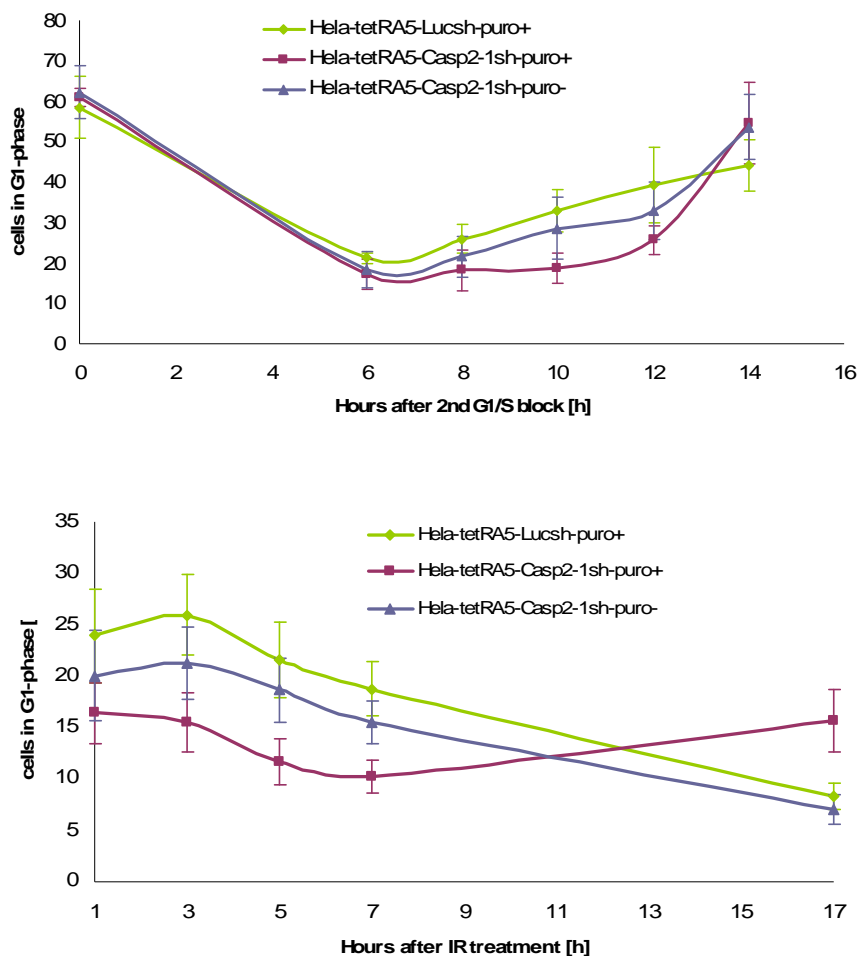
Figure 28: Comparison of the G1-phase of HeLa-tetRA5 RNAi cell lines with and without IR-treatment.
The upper panel shows cells in G1-phase after release from the DTB. Induced caspase 2 RNAi cells show a stronger decrease of cells in G1-phase until 12 hours before increasing again in contrast to controls, which already show an increase of cells in G1-phase 8 hours after the release from the DTB.
Caspase 2 knock-down reveals an increase of cells in G1-phase after DNA damage, indicated by a purple line (lower panel), compared to non-induced caspase 2 and induced Luciferase RNAi cells (mean ± SEM).

5 Conclusion

The aim of my master thesis was to investigate the role of caspase 2 in the cell cycle, particularly in the G2/M checkpoint in response to DNA damage.

We were able to efficiently synchronize HeLa-tetRA5-derived RNAi cells by a double thymidine block, which revealed a better synchronisation following caspase 2 knock-down compared to both controls, non-induced caspase 2 and induced Luciferase RNAi cells, indicated by an efficient block at the G1/S transition of caspase 2 deficient cells in contrast to the controls, which also showed G2-phase cells after a DTB. These data were confirmed by a specific phospho-histone H3 staining that only highlights positive mitotic cells. We therefore

concluded that there may be a difference in checkpoint response in these cell lines due to caspase 2 expression.

By ionizing radiation treatment of cells in G2-phase, we could show that caspase 2 is not required for DNA damage-induced G2/M checkpoint control in Hela-tetRA5-derived RNAi cell lines. However, we could observe an increase of cells in G1-phase following DNA damage just in caspase 2 deficient cells line, which is in line with Sohn *et al.* (2011), who published that untransfected or control siRNA-transfected HCT 116 wild type cells showed significantly lower numbers of BrdU-stained cells after IR treatment compared to caspase 2 siRNA-transfected wild-type cells. Moreover, published data by Shi *et al.* (2009) that caspase 2 deficient, SV-40 immortalized MEFs show significantly more cells in the cell cycle upon DNA damage, are also consistent with our results. In summary, although not essential for the G1/S and G2/M checkpoints, caspase 2 appears to control the tightness of these important and cancer relevant cell cycle transition points.

6 References

1. Alberts, B., Johnson, A., Lewis, J., Raff, M., Roberts, K., Walter, P. (2010) Molekularbiologie der Zelle; Wiley-VCH, pp 1192–1277.

2. Chen, M., Orozco, A., Spencer, D.M., Wang, J. (2002) Activation of initiator caspases through a stable dimeric intermediate, *J. Biol. Chem.* 277, 50761-50767.

3. Donepudi, M., MacSweeney, A., Briand, C., Grutter, M.G. (2003) Insights into the regulatory mechanism for caspase-8 activation. *Mol. Cell* 11, 543-549.

4. Shi, Y. (2002) Mechanisms of caspase activation and inhibition during apoptosis. *Mol. Cell* 9, 459-470.

5. Fischer, U., Janicke, R.U., Schule-Osthoff, K. (2003) Many cuts to ruin: a comprehensive update of caspase substrates. *Cell Death Diff.* 10, 76-100.

6. Tinel, A., Tschopp, J. (2004) The PIDDosome, a protein complex implicated in activation of caspase-2 in response to genotoxic stress. *Science* 304, 843-846.

7. Baliga, B.C., Read, S.H., Kumar, S. (2004) The biochemical mechanism of caspase-2 activation. *Cell Death and Diff.* 11, 1234-1241.

8. McStay, G.P., Salvesen, G.S., Green, D.R. (2008) Overlapping cleavage motif selectivity of caspases: Implications for analysis of apoptotic pathways. *Cell Death Differ.* 15, 322-331.

9. Kumar, S. (2009) Caspase 2 in apoptosis, the DNA damage response and tumour suppression: enigma no more? *Nature* 9, 897-903.

10. Lamkanfi, M., Fewstjens, N., Declercy, W., Vanden Berghe, T. & Vandenabeele, P. (2007) Caspases in cell survival, proliferation and differentiation. *Cell DeathDiff.* 14, 44-55.

11. Bergeron, L. *et al.* (1998) Defects in regulation of apoptosis in caspase-2-deficient mice. *Genes Dev.* 12, 1304-1314.

12. O'Reilly, L.A., Ekert, P., Harvey, N., Marsden, V., Cullen, L., Vaux, D.L., Hacker, G., Magnusson, C., Pakusch, M., Cecconi, F., Kuida, K., Strasser, A., Huang, D.C., Kumar, S. (2002) Caspase-2 is not required for thymocyte or neuronal apoptosis even though cleavage of capsase-2 is dependent on both Apaf-1 and caspase-9. *Cell Death Differ.* 9, 832-841.

13. Baliga, B.C., Colussi, P.A., Read, S.H., Dias, M.M., Jans, D.A., Kumar, S. (2003) Role of prodomain in importin-mediated nuclear localization and activation of caspase-2. *J. Biol. Chem.* 278, 4899-4905.

14. Kumar, S., Tomooka, Y., Noda, M. (1992) Identification of a set of genes with developmentally down-regulated expression in the mouse brain. *Biochem. Biophys. Res. Commun.* 185, 1155-1161.

15. Wang, L., Miura, M., Bergeron, L., Zhu, H., Yuan, J. (1994) *Ich*-1, an *Ice/ced-3*-related gene, encodes both positive and negative regulators of programmed cell death. *Cell* 78, 739-750.

16. Manzl, C., Krumschnabel, G., Bock, F., Sohm, B., Labi, V., Baumgartner, F., Logette, E., Tschopp, J., Villunger, A. (2009) Caspase-2 activation in the absence of PIDDosome formation. *J. Cell Biol.* 185, 291-303.

17. Shi, M., Vivian, C.J., Lee, K.-J., Ge, C., Morotomi-Yano, K., Manzl, C., Bock, F., Sato, S., Tomomori-Sato, C., Zhu, R., Hau, J.S., Swanson, S.K., Washburn, M.P., Chen, D.J., Chen, B.P.C., Villunger, A., Florens, L., Du, C. (2009) DNA-PKcs-PIDDosome: a nuclear caspase-2-activating complex with role in G2/M checkpoint maintenance. *Cell* 136, 508-520.

18. Kraus, G. (2003) Biochemistry of Signal Transduction and Regulation; Wiley-VCH, pp 429-468 & pp 511-532

19. Yuan, J., Shaham, S., Ledoux, S., Ellis, H. M. & Horvitz, H. R. (1993) The C. elegans cell death gene *ced-3* encodes a protein similar to mammalian interleukin-1β -converting enzyme. *Cell* 75, 641–652.

20. Bergeron, L., Perez, G.I., Macdonald, G., Shi, L., Sun, Y., Jurisicova, A., Varmuza, S., Latham, K. E., Flaws, J.A., Salter, J.C.M., Hara, H., Moskowitz, M.A., Li, E., Greenberg, A., Tilly, J.L., Yuan, J. (1998) Defects in regulation of apoptosis in caspase-2-deficient mice. *Genes and Development* 12, 1304–1314.

21. Ho, L. H., Read, S. H., Dorstyn, L., Lambrusco, L., Kumar, S. (2008) Caspase-2 is required for cell death induced by cytoskeletal disruption. *Oncogene* 27, 3393–3404.

22. Kitevska, T., Spencer, D.M.S., Hawkins, C.J. (2009) Caspase-2: controversial killer or checkpoint controller? *Apoptosis* 14, 829-848.

23. Sohn, D., Budach, W., Jänicke, R.U. (2011) Caspase-2 is required for DNA damage-induced expression of the CDK inhibitor p21[WAF1/CIP1]. *Cell Death Differ.* 18 , 1664-1674.